

PROBABILITY DISTRIBUTIONS OF  
THE ZEROS OF RANDOM NOISE

Thesis by

Clarence Rollins Gates

In Partial Fulfillment of the Requirements

For the Degree of

Doctor of Philosophy

California Institute of Technology

Pasadena, California

1951

#### ACKNOWLEDGMENTS

The author wishes to express his appreciation for the kind assistance and encouragement of Dr. Wm. H. Pickering, supervisor of this research. He is also indebted to Stephen O. Rice of the Bell Telephone Laboratories, who suggested the problem in a letter to the author. Further thanks go to Mr. Paul G. Thiene for his valuable suggestions on the design of the apparatus.

## ABSTRACT

A complete expression for the probability distribution of the zero crossing periods of filtered random noise is given. The first term of this expression is evaluated and extended to include narrow, symmetrical spectra. The behavior of the frequency function about the second and further half-periods is investigated.

Apparatus has been designed and constructed which gives directly the distribution function of the zeros of filtered random noise. Distribution functions corresponding to several filters are shown. Correlation between theoretical and experimental distributions is good.

## I. INTRODUCTION

In the last twenty-five years noise theory has risen from comparative insignificance to become an essential element in communications and control systems. Early workers in the field investigated noise sources; Schottky<sup>(1)</sup> reported the shot effect in 1918, and in 1928 Nyquist<sup>(2)</sup> predicted and Johnson<sup>(3)</sup> verified the presence of thermal noise in resistors. Later work was concerned with the relationship between noise voltage and bandwidth<sup>(4)</sup>, with determinations of limitations in sensitivity due to noise<sup>(5), (6)</sup>, and with estimates and measurements of the crest factor.\*<sup>(7)</sup> However advances made in the last decade have been the most significant. The effects of noise in linear and in many non-linear systems have been calculated by Rice<sup>(8)</sup>, Middleton<sup>(9), (10), (11)</sup>, and others<sup>(12)</sup>. Also the noise-minimization problem has been given detailed treatment by Wiener<sup>(13)</sup> and his associates<sup>(14)</sup>. The essential basis for these enormous contributions to noise study has been the application of statistics and probability theory.

Although early workers were aware of the statistical nature of noise, and some preliminary studies were made<sup>(7)</sup>, it was principally through the work of Rice<sup>(15)</sup>, Franz<sup>(16)</sup>, and Wiener<sup>(13), (17)</sup> that a more nearly complete statistical description of noise was made, and a firmer foundation for noise theory laid. Mathematical analyses were made of noise

---

\*This term has now largely been dropped from the literature. It is used to describe the ratio of the highest peaks of a noise voltage to its RMS value.

originating in various sources, notably shot effect in vacuum tubes and the thermal agitation of electrons in resistors. Studies were made of the noise obtained by passing random noise through physical devices. Powerful methods for determining the behavior of noise in non-linear systems were obtained. Relationships between spectra and correlation functions were deduced.

It was during a study, by Stephen O. Rice, of certain properties of noise having a specified spectral distribution, including topics such as the characteristics of the maxima and minima, energy distribution, etc., that the problem of the distribution of the zeros was proposed.<sup>(15)</sup> The problem is as follows: We are given random noise with a specified spectrum. Denote by the random variable  $\tau$  the distance between successive zero crossings of the noise, such as could be measured directly on an oscillograph. What is the distribution of the random variable  $\tau$ ?

If the noise is truly random, having a flat spectrum out to infinite frequency, the solution is quite easy, being related to the Poisson distribution. For any other spectral distribution a solution has not been obtained. If we choose a spectrum which excludes all frequencies but those in a narrow band about  $f_0$ , a partial solution can be obtained. The solution to the narrow band-pass problem is indicated briefly by Rice<sup>(15)</sup>; treatment, in extended form, is given in the following sections. For such a spectrum we would intuitively expect a peak in the frequency function of  $\tau$  at the value

$\tau = \frac{1}{2\delta}$ , the sharpness of the peak depending on the width of the band about  $f_0$ . This result, as will be illustrated, has been verified experimentally.

## II. THEORETICAL DISCUSSION OF THE DISTRIBUTION OF THE ZEROS

### 1. The Solution for Complete Randomness.

We shall say that noise is completely random if knowledge of its magnitude at a certain time yields no information, statistical or otherwise, about its value at any other time; this is equivalent to saying that its (auto)correlation function is zero for all values of the argument other than zero. For such noise we may write

$$P_T(n) = \frac{(\nu T)^n e^{-\nu T}}{n!},$$

where  $P_T(n)$  is the probability of obtaining  $n$  zeros in time  $T$ , and  $\nu$  is the expected number of zeros per unit time.  $P_T(n)$  will be recognized as an ordinary Poisson distribution. Now if we let  $\tau$  equal the time interval between successive zeros, and  $P_0(\tau)d\tau$  the probability of obtaining a zero in  $(\tau, \tau+d\tau)$  if there is one at  $\tau=0$  and none between 0 and  $\tau$ , then

$$\begin{aligned} P_0(\tau)d\tau &= (\text{Probability of a zero in } \tau, \tau+d\tau) \times \\ &\quad (\text{Probability that there is none between}) \\ &= \nu d\tau \times P_\tau(0). \end{aligned}$$

$$\text{Thus } P_0(\tau)d\tau = \nu e^{-\nu\tau}. \quad (1)$$

The characteristic function of  $P_0(\tau)$  is given by

$$Q(t) = \frac{\nu}{\nu - it}$$

and its mean and standard deviation are

$$\sigma = \frac{1}{\nu} ; \quad m = \frac{1}{\nu} .$$

Completely random noise is precisely characterized by a spectrum flat to infinity. In practice we can obtain nearly completely random noise from a spectrum flat to a large frequency  $f_0$  and zero beyond  $f_0$ . The correlation function  $\psi(\tau)$  for such spectra is given as

$$\psi(\tau) = \frac{1}{2\pi\tau} \sin 2\pi f_0 \tau .$$

For increasing  $f_0$ ,  $\psi(\tau)$  becomes more sharply peaked about  $\tau=0$ . Also, the expected number of zeros can easily be calculated for the above spectrum; it will later be shown that  $\nu = f_0$ .

## 2. The Solution for the General Case.

In this section we shall treat random noise having a specified but arbitrary spectrum. For this spectrum consider  $C$ , the class of all curves having zeros at zero and in  $(\tau, \tau+d\tau)$ . If, in  $n$  random samples, we have  $r$  curves which do not cross the axis between zero and  $\tau$ , then we are interested in finding  $\lim_{n \rightarrow \infty} \frac{r}{n} = p_0(\tau) d\tau$ .

We next define the following probabilities:

$p_0(\tau)d\tau$  = the probability of a zero in  $(\tau, \tau+d\tau)$  if there is one at 0;

$p_1(x, \tau)dxd\tau$  = the probability of a zero in  $(\tau, \tau+d\tau)$  and one in  $(x, x+dx)$  if there is one at 0, etc.;

.....  
 $p_n(x_1, x_2, \dots, x_n, \tau) dx_1 dx_2 \dots dx_n d\tau$ .

Now  $p_0(\tau)d\tau$  corresponds to all curves having zeros at 0 and in  $(\tau, \tau+d\tau)$ ; therefore we must subtract from it probabilities corresponding to curves crossing between 0 and  $\tau$ . The integral  $d\tau \int_0^\tau p_1(x, \tau) dx$  is the expected number of curves through 0 and  $(\tau, \tau+d\tau)$  which cross the axis between 0 and  $\tau$ , counting each crossing as a curve. Thus if we take

$$p_0(\tau)d\tau - d\tau \int_0^\tau p_1(x, \tau) dx,$$

we will have accounted for  $C_1$ , the sub-class of curves crossing the axis precisely once between 0 and  $\tau$ . To account for  $C_2$ , the sub-class having two crossings between 0 and  $\tau$ , we must add  $\frac{d\tau}{2} \int_0^\tau \int_0^\tau p_2 dx_1 dx_2$ , since members of  $C_2$  are

counted twice in the  $p_1$  integral and twice in the  $p_2$  integral.

Extending this process, noting that members of  $C_n$  are counted  $\frac{n!}{(n-2)!}$  times by the  $p_m$  integral, and also that

$$n - \frac{n!}{(n-2)!} \cdot \frac{1}{2!} + \dots + \frac{(-1)^n n!}{1} \cdot \frac{1}{n!} = 1,$$

we obtain

$$P_0(\tau) d\tau = p_0 d\tau - d\tau \int_0^\tau p_1 dx_1 + \frac{1}{2!} \int_0^\tau \int_0^\tau p_2 dx_1 dx_2 - \dots,$$

or

$$P_0(\tau) d\tau = \sum_{n=0}^{\infty} \frac{(-1)^n}{n!} \int_0^\tau dx_1 \dots \int_0^\tau dx_n p_n(x_1, \dots, x_n, \tau). \quad (2)$$

This may easily be checked for random events. In this case we have  $p_0 = \nu$ ,  $p_1 = \nu^2 \dots$ , and

$$\begin{aligned} P_0(\tau) &= \sum_{n=0}^{\infty} \frac{(-1)^n}{n!} \nu^{n+1} \tau^n \\ &= \nu e^{-\nu\tau} \end{aligned} \quad (1)$$

It now remains to obtain the  $p_0, p_1, \dots$ .

Expected Number of Zeros. We must first evaluate  $P(\tau)d\tau$ , which is defined to be the probability of obtaining a zero in  $(\tau, \tau+d\tau)$ . This result was first obtained by Rice<sup>(15)</sup>, and is presented here in order that the method may later be used. Let  $F(x)$  represent our noise function. Denote

$$\xi = F(x),$$

$$\eta = \frac{\partial F}{\partial x}.$$

It has been fairly well established, through application of the Central Limit Theorem, that  $\xi$  and  $\eta$  are normally distributed. (Strictly speaking we should use  $\xi = F(a_1, \dots, a_n, x)$ , where the  $a$ 's are random variables which are fixed for a given  $F$ . We refer the reader to Rice.) Next consider the set  $S$  of all  $\xi$  and  $\eta$  such that

$$\text{either } -\eta, dx, < \xi, < 0$$

$$\text{or } -\eta, dx, > \xi, > 0$$

If, in  $\xi\eta$  space, the point  $(\xi, \eta)$  is in the set  $S$ , then we will have an axis crossing in  $(x, x+dx)$ . Thus if  $f(\xi, \eta) = p(\xi, \eta; x)$  is the joint frequency function of  $\xi$  and  $\eta$ , we have

$$P(x) dx = \int_S p(\xi, \eta; x) d\eta d\xi = \int_0^\infty \int_{-\eta dx}^0 p d\eta d\xi + \int_{-\infty}^0 \int_0^{-\eta dx} p d\eta d\xi.$$

Since  $dx$  is presumed small, it follows that

$$P(x) dx = dx \int_0^\infty p(0, \eta; x) d\eta - dx \int_{-\infty}^0 p(0, \eta; x) d\eta,$$

$$\text{or } P(x) = \int_{-\infty}^\infty |\eta| p(0, \eta; x) d\eta.$$

If we assume that  $\overline{F(x)} = 0$ , we may compute the second-order central moments as follows:

$$\lambda_{11} = E(\xi^2) = \lim_{T \rightarrow \infty} \frac{1}{T} \int_0^T F^2(\eta) dx = \psi(0)$$

$$\lambda_{22} = E(\eta^2) = \lim_{\tau \rightarrow 0} E(\eta_x \eta_{x+\tau}) = \lim_{\tau \rightarrow 0} \lim_{T \rightarrow \infty} \frac{1}{T} \int_0^T F'(x+\tau) F'(x) dx,$$

$$\lambda_{22} = -\psi''(0)$$

$$\begin{aligned}\lambda_{12} &= E(\xi \eta) = \lim_{T \rightarrow \infty} \frac{1}{T} \int_0^T F'(x) F(x) dx \\ &= \psi'(0) = 0\end{aligned}$$

Thus

$$P(\xi, \eta; \kappa) = \frac{1}{2\pi\sqrt{\Lambda}} e^{-\frac{1}{2\Lambda} (\lambda_{11}\xi^2 + \lambda_{22}\eta^2)}$$

and

$$\Lambda = \begin{pmatrix} \lambda_{11} & \lambda_{12} \\ \lambda_{21} & \lambda_{22} \end{pmatrix} = \begin{pmatrix} \psi(0) & 0 \\ 0 & -\psi''(0) \end{pmatrix}.$$

Further,

$$P(0, \eta; \kappa) = \frac{1}{2\pi(-\psi_0'')}^{\frac{1}{2}} e^{-\frac{\eta^2}{2\psi_0''}}$$

$$\text{Thus } P(x) = \frac{1}{\pi} \left( \frac{-\psi_0''}{\psi_0''} \right)^{\frac{1}{2}}. \quad (3)$$

$P(x)$  also represents the expected number of zeros per second.

Determination of  $p_n(x_1, x_2 \dots x_n, \tau)$ . We wish to find  $p_n(x_1, x_2 \dots x_n, \tau)$ , the probability of having zeros in  $(x_1, x_1+d\tau) \dots (x_n, x_n+d\tau)$  when it is known there is a zero at 0. Let  $E_{x_i}^+$  denote the event of a zero at  $x_i$  with positive slope,  $E_{x_i}^-$  a zero at  $x_i$  with negative slope, etc. Then the probability we want is

$$P(E_{x_1}^{\pm} E_{x_2}^{\pm} \dots E_{x_n}^{\pm} | E_0^{\pm})$$

Clearly

$$P(E_{x_1}^{\pm} \dots E_{x_n}^{\pm} | E_0^{\pm}) = P(E_{x_1}^{\pm} \dots E_{x_n}^{\pm} | E_0^+),$$

which is easier to evaluate. Further,

$$P(E_{x_1}^{\pm} \dots E_{x_n}^{\pm} | E_0^+) = \frac{P(E_{x_1}^{\pm} \dots E_{x_n}^{\pm} E_0^+)}{P(E_0^+)}$$

Consider next the set S having subsets

(1)	(2)	(3)
$-\eta_0 dx_0 < \xi_0 < 0$	$-\eta_0 dx_0 < \xi_0 < 0$	$-\eta_0 dx_0 < \xi_0 < 0$
$-\eta_1 dx_1 < \xi_1 < 0$	$-\eta_1 dx_1 > \xi_1 > 0$	$-\eta_1 dx_1 > \xi_1 > 0$
$-\eta_2 dx_2 < \xi_2 < 0$	$-\eta_2 dx_2 < \xi_2 < 0$	$-\eta_2 dx_2 > \xi_2 > 0$
. . .	. . .	. . .
$-\eta_{n+1} dx_{n+1} < \xi_{n+1} < 0$	$-\eta_{n+1} dx_{n+1} < \xi_{n+1} < 0$	$-\eta_{n+1} dx_{n+1} < \xi_{n+1} < 0$

To construct the subsets we keep the 0th inequality fixed and vary the remaining ones in all possible ways. This results in  $2^{n+1}$  subsets in S. Each of the subsets represents one of the mutually exclusive ways in which  $P(E_{x_1}^{\pm} \dots E_{x_n}^{\pm} E_0^+)$  can happen. If the frequency function is given by

$$f(\xi_0, \xi_1, \dots, \xi_{n+1}, \eta_0, \dots, \eta_{n+1}),$$

then

$$P(E_{x_1}^{\pm} \dots E_{x_n}^{\pm} E_0^+) = \int_S f dS = \sum_{i=1}^{n+1} \int_{S_i} f dS$$

The first term of the summation is

$$\int_0^{\infty} d\eta_0 \int_{-\eta_0 dx_0}^0 d\xi_0 \cdot \dots \cdot \int_0^{\infty} d\eta_{n+1} \int_{-\eta_{n+1} dx_{n+1}}^0 d\xi_{n+1} f$$

Remembering that  $dx_0, dx_1, \dots, dx_{n+1}$  are small, we may write

$$\frac{P(E_{x_1}^{\pm} \dots E_0^+)}{dx_0 \dots dx_{n+1}} = \sum (-1)^n \int_0^{\infty} \int \dots \int \eta_0 \eta_1 \dots \eta_{n+1} f(0, \dots, 0, \eta_0, \dots, \eta_{n+1}) d\eta_0 \dots d\eta_{n+1}$$

where the second  $n$  integrals in each term of the sum are the  $2^{n+1}$  possible arrangements of  $\int_0^\infty$  and  $\int_{-\infty}^0$  taken  $n+1$  at a time, and  $r$  is the total number of integrals having lower limits of  $(-)$ infinity in any term.

We may evaluate the elements of the moment matrix as indicated in the preceding section. Carrying out these operations leads to the moment matrix  $\Lambda$ , shown in Fig. 1. The matrix is of order  $(2n+4)(2n+4)$ .

Once the moment matrix is determined we can find the frequency function as follows:

$$f(x_0, \dots, x_{n+1}, \eta_0, \dots, \eta_{n+1}) = \frac{1}{(2\pi)^{n+2} \sqrt{\Lambda}} e^{-\frac{1}{2\Lambda} \sum_{j,k} \Lambda_{j,k} x_j x_k} ;$$

$$f(0, \dots, 0, \eta_0, \dots, \eta_{n+1}) = \frac{1}{(2\pi)^{n+2} \sqrt{\Lambda}} e^{-\frac{1}{2\Lambda} \sum_{j,k} \Lambda_{j,k} \eta_j \eta_k} . \quad (4)$$

Note that  $\Lambda_{j,k}$  is the cofactor of  $\Lambda_{j,k}$  in  $\Lambda$ , and  $j$  and  $k$  in the latter summation run from  $n+3$  to  $2n+4$ . ( $\eta_i \rightarrow \eta_{i+n+2}$ ).

Also  $P(E_0^+) = \frac{1}{2} P(E_0^\pm) = \frac{1}{2\psi} \left( \frac{-\psi_0''}{\psi_0''} \right)^{\frac{1}{2}}$ . This completes the formal determination of  $P_0(\tau)$ .

Reduction of  $p_0(\tau)$ . It is possible to simplify further the expression for  $p_0(\tau)$ . Using (3) and (4) we obtain

$$P_0(E_0^+ E_\tau^\pm) = \int_0^\infty \int_0^\infty \eta_0 \eta_\tau f d\eta_0 d\eta_\tau - \int_0^\infty d\eta_0 \int_{-\infty}^0 f d\eta_\tau$$

where

$$f = f(0, 0, \eta_0, \eta_\tau) = \frac{1}{(2\pi)^2 \sqrt{\Lambda}} \exp -\frac{1}{2\Lambda} (\Lambda_{33} \eta_0^2 + 2\Lambda_{34} \eta_0 \eta_\tau + \Lambda_{44} \eta_\tau^2)$$

and

$$\Lambda = \begin{pmatrix} \psi_0 & \psi_\tau & 0 & \psi_\tau' \\ \psi_\tau & \psi_0 & -\psi_\tau' & 0 \\ 0 & -\psi_\tau' & -\psi_0'' & -\psi_\tau'' \\ \psi_\tau' & 0 & -\psi_\tau'' & -\psi_0'' \end{pmatrix} .$$

$\psi_0$	$\psi_{x_1}$	$\psi_{x_2}$	$\psi_{x_3}$			$\psi_{x_n}$	$\psi_{x_r}$	0	$\psi'_{x_1}$	$\psi'_{x_2}$	$\psi'_{x_3}$			$\psi'_{x_n}$	$\psi'_{x_r}$
$\psi_{x_1}$	$\psi_0$	$\psi_{x_2-x_1}$	$\psi_{x_3-x_1}$			$\psi_{x_n-x_1}$	$\psi_{x_r-x_1}$	$\psi'_{-x_1}$	0	$\psi'_{x_2-x_1}$	$\psi'_{x_3-x_1}$				$\psi'_{x_r-x_1}$
$\psi_{x_2}$	$\psi_{x_2-x_1}$	$\psi_0$	$\psi_{x_3-x_2}$			$\psi_{x_n-x_2}$	$\psi_{x_r-x_2}$	$\psi'_{-x_2}$	$\psi'_{x_1-x_2}$	0	$\psi'_{x_3-x_2}$				
			$\psi_0$								0				
		(I)		$\psi_0$							(II)		0		
					$\psi_0$								0		
						$\psi_0$	$\psi_{x_n}$							0	$\psi'_{x_r-x_n}$
							$\psi_0$							$\psi'_{x_n-x_r}$	0
0	$\psi'_{-x_1}$	$\psi'_{-x_2}$						$-\psi_0''$	$-\psi_{x_1}''$	$-\psi_{x_2}''$					
$\psi'_{x_1}$	0	$\psi'_{x_1-x_2}$						$-\psi_{x_1}''$	$-\psi_0''$	$-\psi_{x_2-x_1}''$	$-\psi_{x_3-x_1}''$				
$\psi'_{x_2}$	$\psi'_{x_2-x_1}$	0								$-\psi_0''$	$-\psi_{x_1-x_2}''$				
			0												
			(IV)								(III)				
															$-\psi_0''$
															$-\psi_0''$

$$a_{ij}^I = \psi(x_{i-1} - x_{j-1}) \quad \bar{a}_{ij}^III = -\psi''(x_{i-1} - x_{j-1})$$

$$a_{ij}^I = a_{ji}^I \quad \bar{a}_{ij}^III = a_{ji}^III$$

$$a_{ij}^II = \psi(x_{i-1} - x_{j-1}) \quad \bar{a}_{ij}^IV = a_{ji}^IV = -a_{ij}^II$$

$$a_{ij}^II = -a_{ji}^II \quad \bar{a}_{ij}^IV = -a_{ji}^IV$$

Fig. 1. The  $\Lambda$  Matrix.

It can easily be shown that  $\Lambda_{33} = \Lambda_{44}$ .

Next let

$$x = \left( \frac{\Lambda_{33}}{2\Lambda} \right)^{\frac{1}{2}} \eta_0,$$

$$y = - \left( \frac{\Lambda_{33}}{2\Lambda} \right)^{\frac{1}{2}} \eta_1.$$

Substituting yields

$$P(E_0^+ E_1^+) = \frac{\Lambda^{\frac{3}{2}}}{\pi^2 \Lambda_{33}^2} \left( \int_0^{\infty} \int_0^{\infty} xy e^{-x^2 y^2 - 2 \frac{\Lambda_{34}}{\Lambda_{33}} xy} dx dy + \int_0^{\infty} \int_0^{\infty} xy e^{-x^2 y^2 + 2 \frac{\Lambda_{34}}{\Lambda_{33}} xy} dx dy \right).$$

Using

$$\int_0^{\infty} \int_0^{\infty} xy e^{-x^2 y^2 - 2xy \cos \theta} dx dy = \frac{1}{4} \sec^2 \theta (1 - \theta \cot \theta),$$

we have

$$P_+(E_1^+ E_0^+) = \frac{\Lambda^{\frac{3}{2}}}{2\pi^2 (\Lambda_{33}^2 - \Lambda_{34}^2)} \cdot (1 + k \tan^{-1} k),$$

where  $k = \frac{\Lambda_{34}}{(\Lambda_{33}^2 - \Lambda_{34}^2)^{\frac{1}{2}}}$ .

Also, by Jacobi's Theorem (18),

$$\begin{vmatrix} \Lambda_{33} & \Lambda_{34} \\ \Lambda_{43} & \Lambda_{44} \end{vmatrix} = \begin{vmatrix} \psi_0 & \psi_1 \\ \psi_1 & \psi_0 \end{vmatrix} \Lambda,$$

and thus

$$\Lambda^{\frac{3}{2}} = \frac{(\Lambda_{33}^2 - \Lambda_{34}^2)^{\frac{3}{2}}}{(\psi_0^2 - \psi_1^2)^{\frac{3}{2}}}.$$

Using  $P(E_0^+) = \frac{1}{2\pi} \left( \frac{-\psi_0''}{\psi_0} \right)^{\frac{1}{2}}$ , we have

$$p_0(z) = \frac{1}{2\pi} \left( \frac{\psi_0}{-\psi_0''} \right)^{\frac{1}{2}} \frac{(\Lambda_{33}^2 - \Lambda_{34}^2)^{\frac{1}{2}}}{(\psi_0^2 - \psi_T^2)^{\frac{3}{2}}} (1 + k \tan^{-1} k). \quad (5)$$

### 3. Solution for Narrow Band-pass Filter.

In this section we shall compute approximately the distribution of the zeros for a narrow band-pass filter. We shall assume that the first term of Eq. (1) adequately represents the frequency function, which is equivalent to saying that the probability of more than one axis crossing in the interval is negligible.

Our spectrum  $\omega(f)$  will be given by

$$\begin{aligned}\omega(f) &= \omega_0, \quad f_a \leq f \leq f_b; \\ &= 0, \quad \text{elsewhere.}\end{aligned}$$

It is easily shown that  $P_0$  is independent of any constant multiplier of the spectrum; therefore we may take  $\omega_0=1$ .

Now

$$\psi(r) = \int_0^{\omega} \omega(f) \cos 2\pi f r df$$

If we let  $\alpha = \pi r f_0$  and  $Q = \frac{f_0}{f_b - f_a}$  we get

$$\psi_r = \frac{1}{\alpha} \sin \frac{\alpha}{Q} \cos 2\alpha$$

$$\psi_r' = \frac{\pi}{\alpha Q} \cos \frac{\alpha}{Q} \cos 2\alpha - \frac{2\pi}{\alpha} \sin \frac{\alpha}{Q} \sin 2\alpha - \frac{\pi}{\alpha} \psi_r$$

$$-\psi_r'' = \left( \frac{\pi^2}{Q^2} + 4\pi^2 \right) \psi_r + \frac{2\pi}{\alpha} \psi_r' + \frac{4\pi^2}{Q\alpha} \cos \frac{\alpha}{Q} \sin 2\alpha.$$

Also

$$\psi_0 = \frac{1}{Q}$$

$$\psi_0' = 0$$

$$\psi_0'' = -\frac{4\pi^2}{3Q} \left( 3 + \frac{1}{4Q^2} \right).$$

Note further that

$$\Lambda_{33} = -\psi_0^2 \psi_0'' - \psi_0 \psi_r'^2 + \psi_r^2 \psi_0'' ;$$

$$\Lambda_{34} = \psi_0^2 \psi_r'' + \psi_r \psi_r'^2 - \psi_r \psi_r'' .$$

Investigation of  $\Lambda_{33}$  and  $\Lambda_{34}$  reveals that both quantities are very close to zero. Therefore in their evaluation it is more practical to use approximate methods. To do this we use the series expansions for the trigonometric terms in the correlation function and its derivatives, assume that  $\frac{\alpha}{Q} \ll 1$ , and retain only the first few terms. Carrying out this procedure yields

$$\Lambda_{33} \cong \frac{\pi^2}{3Q^5} (\sin^2 2\alpha + 4\alpha^2 - 4\alpha \sin 2\alpha \cos 2\alpha)$$

$$\Lambda_{34} \cong \frac{\pi^2}{3Q^5} (-\sin^2 2\alpha \cos 2\alpha - 4\alpha^2 \cos 2\alpha + 4\alpha \sin 2\alpha) .$$

Substitution into (5), using  $f_0(\alpha) = \frac{p_0(\alpha)}{\pi f_0}$  in order that we shall still have a distribution, gives us

$$f_0(\alpha) = \frac{1}{6\pi Q^2} \frac{|\sin 2\alpha (\sin^2 2\alpha - 4\alpha^2)|}{(\sin^2 2\alpha + \frac{\alpha^2}{3Q^2} \cos^2 2\alpha)^{\frac{3}{2}}} \cdot (1 + k \tan^{-1} k) .$$

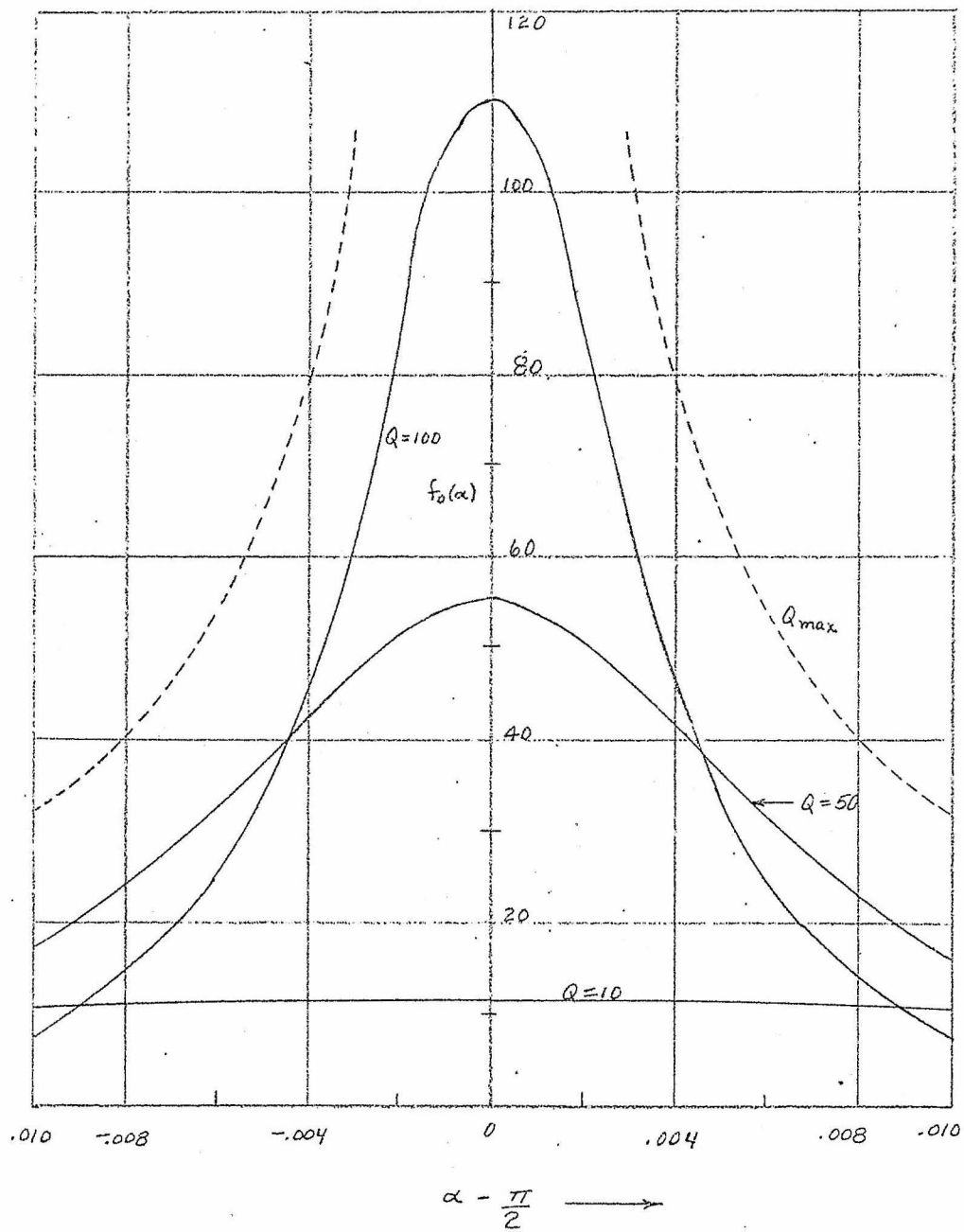
For  $\alpha$  near  $\frac{n\pi}{2}$  the above expression reduces to

$$f_0(\alpha) = \frac{\alpha (n\pi - \alpha)}{3Q^2 \left[ \frac{\alpha^2}{3Q^2} + 4 \left( \alpha - \frac{n\pi}{2} \right)^2 \right]^{\frac{3}{2}}} . \quad (6)$$

Note that  $f_0(\frac{n\pi}{2}) = n f_0(\frac{n\pi}{2})$ .

In Fig. 2 Eq. (6) is plotted for  $n=1$  and several values of  $Q$ . It is seen that  $f_0(\frac{n\pi}{2}) = \frac{2\sqrt{3}}{\pi} Q$ .

Properties of  $f_0(\alpha)$ . ( $n=1$ ). Let us next determine cer-

Fig. 2.  $f_0(\alpha)$ .

tain of the statistical properties of our approximation to  $f_0(\alpha)$  given in Eq. (6). The mean, of course, is  $\frac{\pi}{2}$ . The standard deviation  $\sigma$  is given by

$$\sigma^2 = E\left(\alpha - \frac{\pi}{2}\right)^2 = \frac{\pi^2}{96Q^2} (1 + \ln 48 + 2 \ln Q). \quad (7)$$

A plot of  $\sigma$  versus  $Q$  is given in Fig. 3.

For a given value of  $|\alpha - \frac{\pi}{2}|$  there will be a certain  $Q$  giving a maximum value of  $f_0(\alpha)$ . Using the following approximation to Eq. (6):

$$f_0(\alpha) = \frac{\pi^2}{12Q^2 \left[ \frac{\pi^2}{12Q^2} + 4\left(\alpha - \frac{\pi}{2}\right)^2 \right]^{\frac{3}{2}}}, \quad (8)$$

we find by differentiation that

$$Q_{\max.} = \frac{\pi}{4|\alpha - \frac{\pi}{2}| \sqrt{6}}.$$

$Q_{\max.}$  is indicated in Fig. 2 by the dotted curve.

The "Q" of the frequency function is defined as for a resonance curve. It is without obvious statistical significance, but has been useful in the experimental work. We

wish to find  $\alpha_1$ , then, such that  $\frac{1}{\sqrt{2}} f_0\left(\frac{\pi}{2}\right) = f_0(\alpha_1)$ .

Solving gives

$$\alpha_1 - \frac{\pi}{2} = \frac{\pi}{2Q\sqrt{6}} \left( \frac{2^{\frac{1}{3}} - 1}{2} \right)^{\frac{1}{2}}.$$

Thus

$$\Delta\alpha = 2 \left( \alpha_1 - \frac{\pi}{2} \right),$$

and

$$Q' = \frac{\alpha}{\Delta\alpha} = \frac{\sqrt{3} Q}{(2^{\frac{1}{3}} - 1)^{\frac{1}{2}}} = 3.396 Q.$$

Expected Number of Zeros. From Eq. (3) we may calculate the expected number of zeros for the narrow band-pass filter.

$$\frac{1}{\pi} \left( \frac{-\psi_0''}{\psi_0} \right)^{\frac{1}{2}} = 2 f_0 \left( 1 + \frac{1}{12Q^2} \right)^{\frac{1}{2}} .$$

For  $Q$  tending to infinity we obtain  $2f_0$ , as expected.

The expected number of zeros for noise flat to  $f_0$ , mentioned at the close of section II-1, can now be found. For this spectrum

$$\psi(f) = \int_0^{\infty} \omega(f) \cos 2\pi f \tau \, df = \frac{\omega_0}{2\pi\tau} \sin 2\pi f_0 \tau .$$

Now

$$\psi_0 = \omega_0 f_0 .$$

and

$$\psi_0'' = -4\pi^2 f_0^3 \omega_0 .$$

Thus

$$\frac{1}{\pi} \left( \frac{-\psi_0''}{\psi_0} \right)^{\frac{1}{2}} = f_0 .$$

Non-rectangular Filter Characteristic. In obtaining

Eq. (8) for  $f_0(\alpha)$  we could have used

$$f_0(\alpha) = \frac{1}{4\pi^2} \cdot \frac{\Lambda_{34}}{(\psi_0^2 - \psi_\tau^2)^{\frac{3}{2}}} . \quad (9)$$

To get Eq. (9) from Eq. (5) note that  $\Lambda_{33}$  and  $\Lambda_{34}$  are approximately equal, and that  $\tan^{-1} k \cong \frac{\pi}{2}$  for  $\alpha$  near  $\frac{\pi}{2}$ . Now if

$$\psi_\tau = \varrho(\alpha) \cos 2\alpha ,$$

and

$$\varrho(\alpha) = \varrho_0 + \frac{\alpha^2}{2} \varrho_0'' + \dots ,$$

then

$$\psi_0^2 - \psi_\tau^2 \cong -\varrho_0'' \varrho_0 \frac{\pi^2}{4} \left[ 1 + \frac{16}{\pi^2} \cdot \frac{\varrho_0}{-\varrho_0''} \left( \alpha - \frac{\pi}{2} \right)^2 \right]$$

and  $\Lambda_{34} = \pi^4 \omega_0^2 \omega_0''$ .

Substituting yields

$$f_0(\alpha) = \frac{2}{\pi} \left( \frac{\omega_0}{-\omega_0''} \right) \frac{1}{\left[ 1 + \frac{16}{\pi^2} \frac{\omega_0}{-\omega_0''} \left( \alpha - \frac{\pi}{2} \right)^2 \right]^{\frac{3}{2}}}$$

For the narrow rectangular filter we have

$$\omega(\alpha) = \frac{1}{\alpha} \sin \frac{\alpha}{Q}$$

$$\frac{\omega_0}{-\omega_0''} = 3Q^2$$

Substituting this value in Eq. (8) gives Eq. (9). But suppose we have

$$\omega(\alpha) = \sum_{i=1}^n \frac{A_i}{\alpha} \sin \frac{\alpha}{Q_i}$$

Then

$$\frac{\omega_0}{-\omega_0''} = \frac{3 \sum A_i/Q_i}{\sum A_i/Q_i^3}$$

In this way we can get the frequency function corresponding to any spectrum which can be represented as the sum of a finite number of rectangular spectra of arbitrary amplitudes and widths, all having the same mid-band frequency. To a fair approximation this includes all symmetrical spectra. The assumption that the frequency is near  $f_0$  and that all of the  $Q_i$ 's are large is still in force.

An equivalent  $Q$  can be defined as follows:

$$Q_e^2 = \frac{\sum A_i/Q_i}{\sum A_i/Q_i^3} \quad (10)$$

A filter having this  $Q$  would produce precisely the same distribution of zeros as would the filter indicated by the summation.

For  $n=2$  we have

$$Qe^{-2} = Q_1^2 (1 - r)$$

where

$$r = \frac{(1 - g_{12}^2) a_{12}}{g_{12}^3 + a_{12}}$$

and

$$a_{12} = \frac{A_2}{A_1} ; \quad g_{12} = \frac{Q_2}{Q_1} .$$

Fig. 4 shows  $r$  as a function of  $a_{12}$  and  $g_{12}$ .

The difference of two spectra represents a double band-pass filter. For example, if

$$Q = \frac{1}{\alpha} \sin \frac{\alpha}{Q_a} - \frac{1}{\alpha} \sin \frac{\alpha}{Q_b}$$

then

$$\begin{aligned} &= 1, \quad f_1 - \frac{\Delta f}{2} < f < f_1 + \frac{\Delta f}{2} \\ &= 1, \quad f_2 - \frac{\Delta f}{2} < f < f_2 + \frac{\Delta f}{2} \\ &= 0 \text{ elsewhere,} \end{aligned}$$

where

$$Q_a = \frac{f_0}{\delta f + \Delta f} ; \quad Q_b = \frac{f_0}{\delta f - \Delta f}$$

and

$$f_0 = \frac{f_1 + f_2}{2} .$$

Then

$$Qe^{-2} = \frac{Q^2}{3 \frac{Q}{\alpha} + 1}$$

where

$$Q = \frac{f_0}{\Delta f}$$

and

$$\alpha = \frac{f_0}{\delta f} .$$

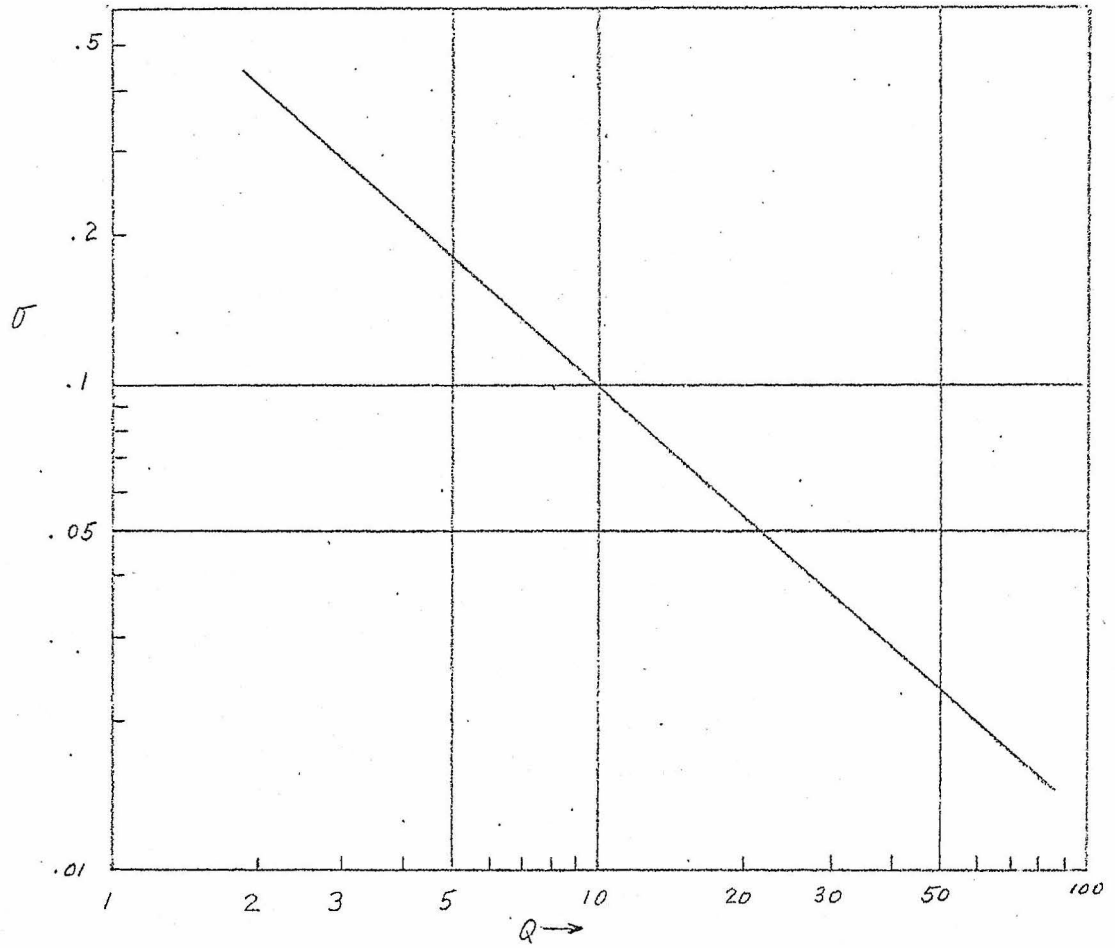


Fig. 3. The standard deviation.

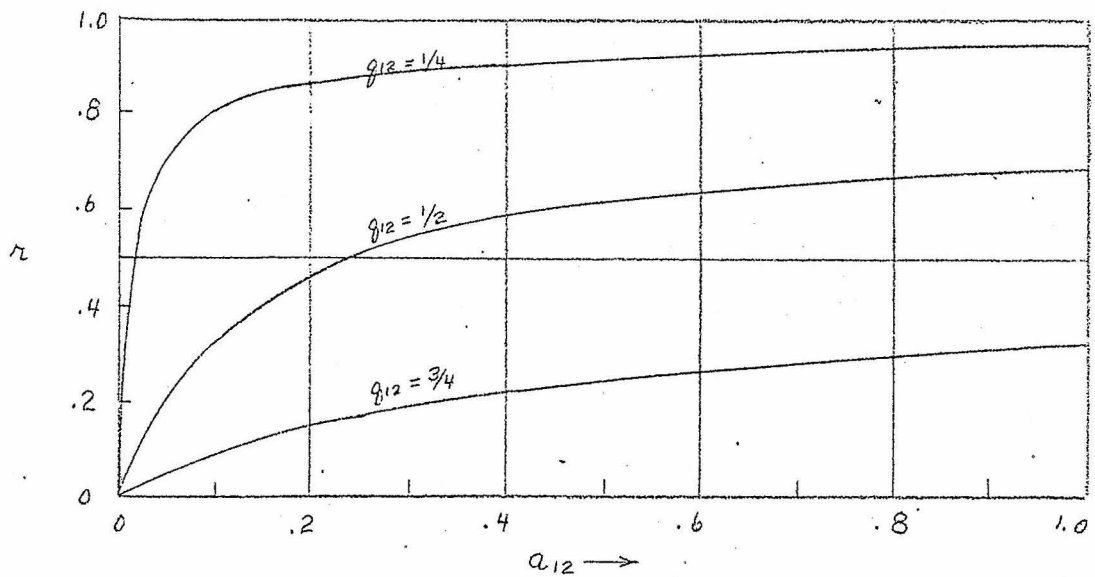


Fig. 4.  $r$  as a function of  $a_{12}$ ,  $q_{12}$ .

## III. THE MEASUREMENT SYSTEM

In the preceding section we saw that the first term of the series which presumably represents the frequency function for the distribution of the zeros could be approximated, although with some difficulty, for the special case of a narrow rectangular band-pass filter. It appears that with methods now available the remaining terms of the series cannot be evaluated, although possibly the second could be determined with a large-scale computer. In order to check the validity of the first term as an approximation to the series (for the narrow band-pass filter), and also to obtain an actual distribution of zeros for noise of a certain known spectrum, an electronic system has been designed and constructed which gives directly the distribution function of the zero-crossing periods corresponding to noise of arbitrary, known spectra.

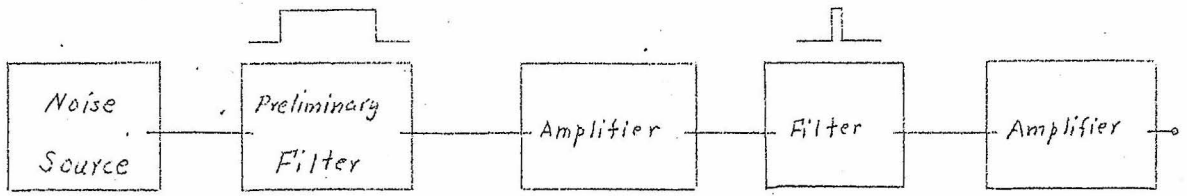
In the measurement system flat random noise is fed through a narrow band-pass filter. The filter output is clipped and differentiated, giving positive pulses for zeros of positive slope, and negative pulses for zeros of negative slope. These pulses are then inverted, clipped, and recombined to give a positive pulse for each zero. The positive pulses are used to generate a sawtooth timing waveform; this timing waveform has constant slope and is triggered by each successive pulse. Next the sawtooth wave is clipped at a specified voltage level corresponding to a certain rise time,

and all surviving peaks of the sawtooth wave are differentiated. The resultant pulses are then shaped and counted. In this way we obtain a measure of all zero-crossing periods greater than a given value; the distribution function is given as an output. The central feature of this system is the sawtooth timing waveform which essentially changes a time measurement to an amplitude measurement.

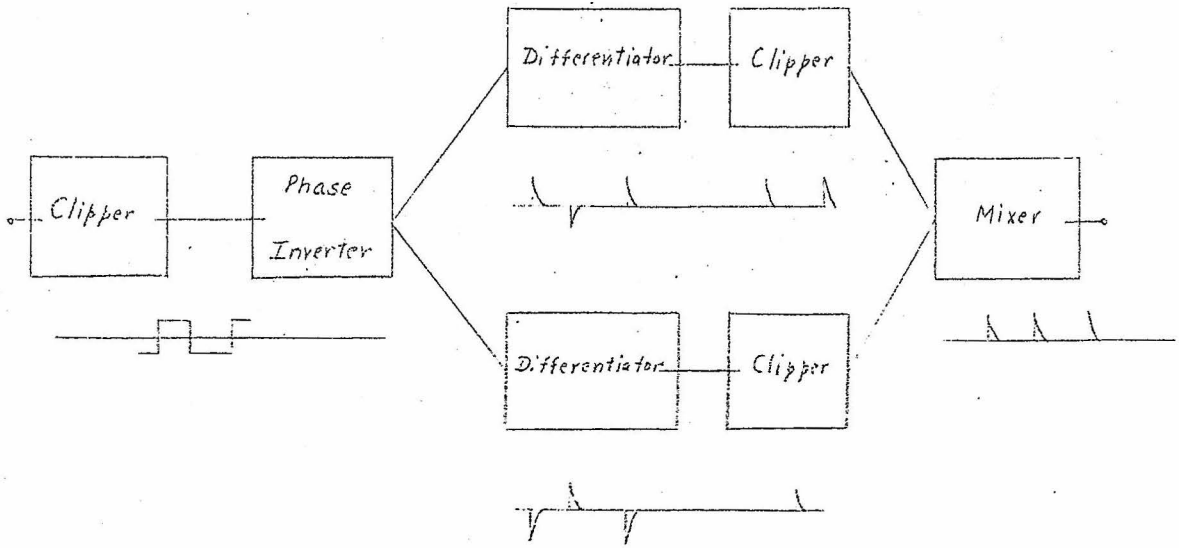
A block diagram of the system is given in Fig. 5, together with typical waveforms illustrating the operations. The apparatus has been sub-divided into three units, each of which occupies a separate chassis.

Discussion of Circuits. The complete circuit diagrams corresponding to the block diagram of Fig. 5 are given on the following pages. Fig. 6 shows the noise source and the preliminary filter and amplifiers. The noise source is a thyratron operating in the conducting state. Its spectrum is flat from near zero frequency to 200 KC. The RMS noise voltage output is .05 volts to .20 volts, depending on the grid voltage. The next stage is a cathode follower which feeds a band-pass filter combination made up of a low-pass and a high-pass filter separated by a second cathode follower. The filter passes from 15 KC to 25 KC; its purpose is to remove the very high and the very low frequencies. A triode amplifier with gain control completes this portion of the circuit.

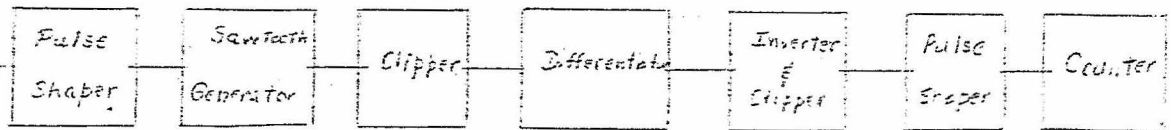
In Fig. 7 we have the spectrum-shaping filter and the output amplifiers. The filters are three cascode bridged-T



UNIT I.



UNIT II.



UNIT III.

Fig. 5. Block diagram.

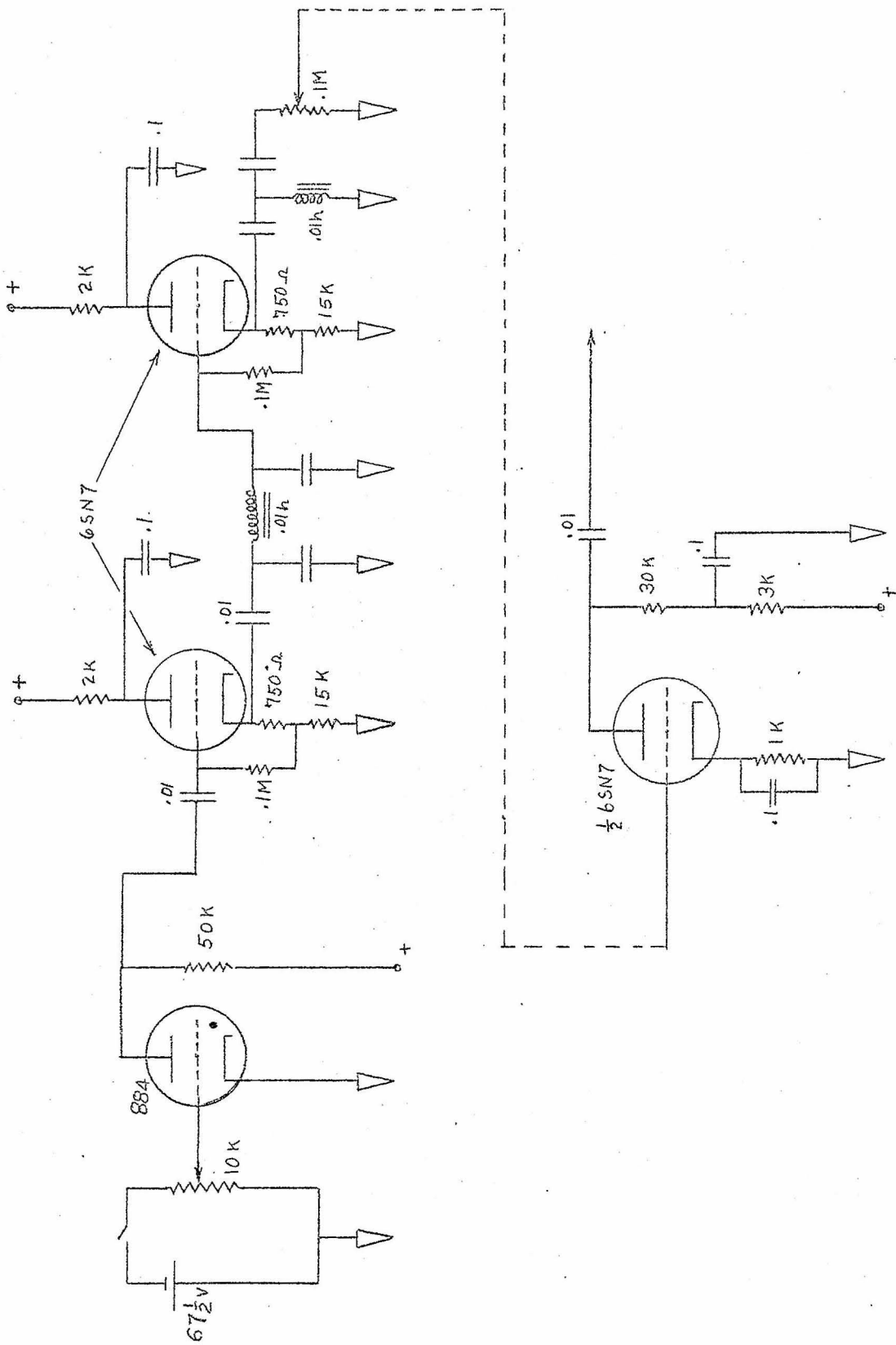


FIG. 6. Noise source, first filter, and amplifier.

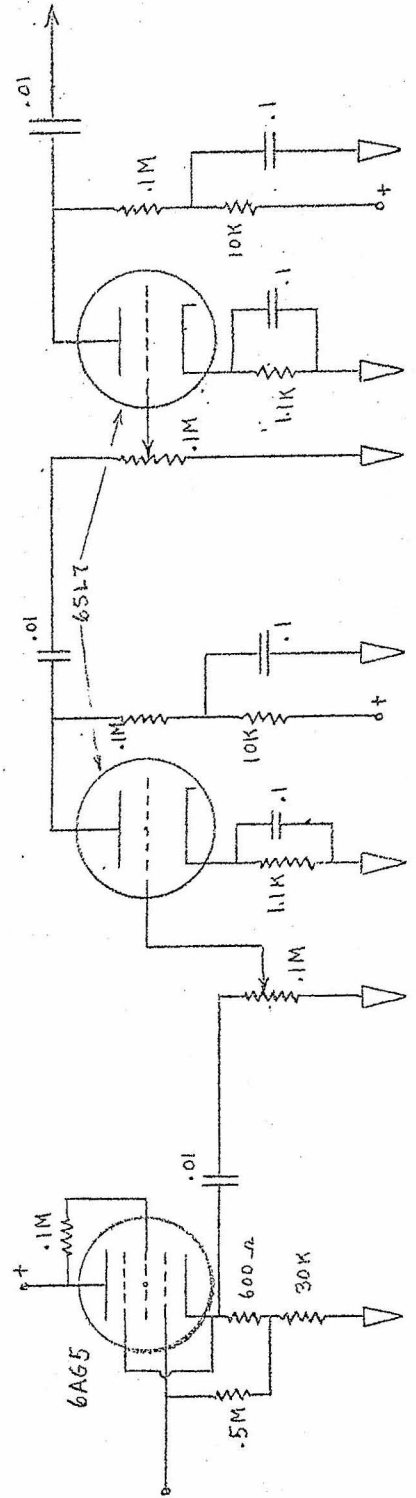
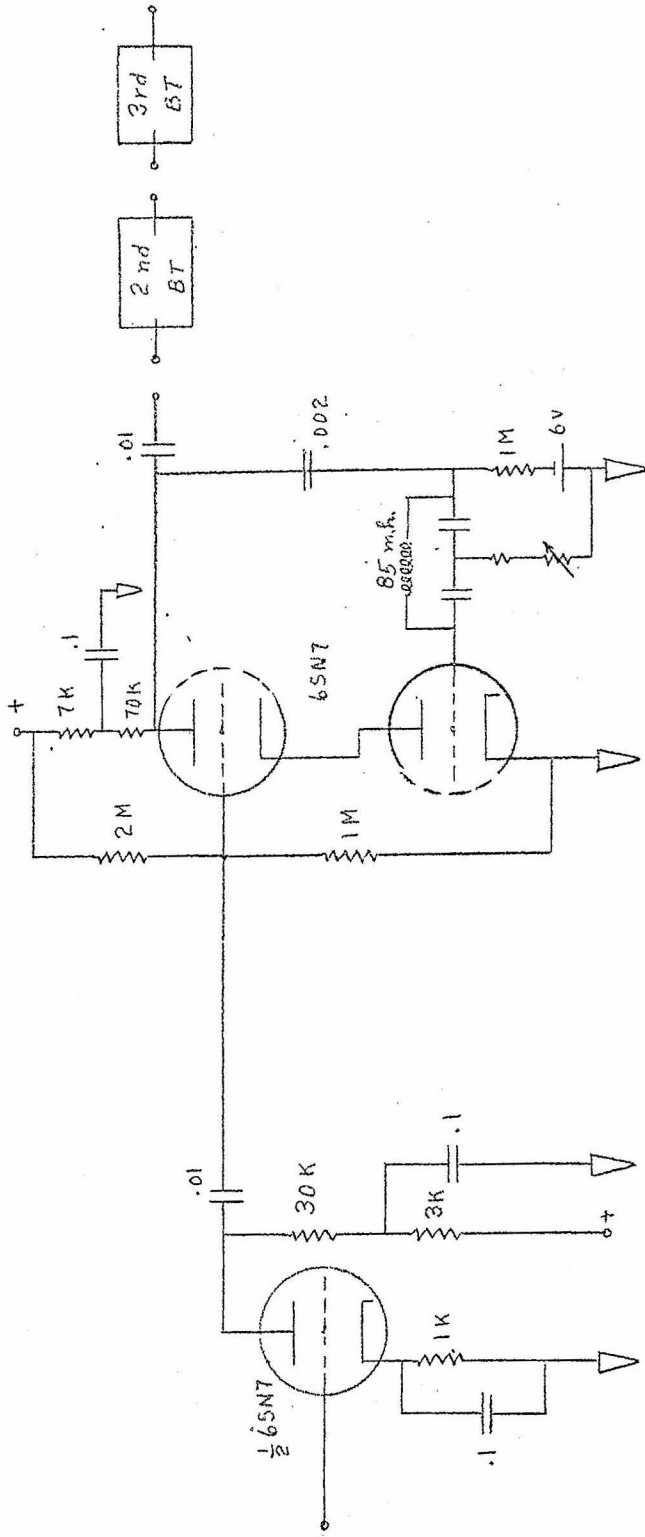


Fig. 7. Bridged-T filters and output amplifiers.

filters<sup>(19)</sup> which may be used individually or in series. The bridged-T has a null frequency characteristic, and when placed in a negative feedback loop results in high selectivity. The resultant  $Q$  is given by  $Q = \frac{1}{2} Q_L G$ , where  $Q_L$  is the  $Q$  of the inductance and  $G$  is the loop gain. We may adjust  $Q_L$  by adding resistance in the inductance branch, and the mid-band frequency is varied by changing the condenser values. A parallel-T circuit was also considered, but its  $Q$  is less by a factor of  $Q_L/4$ . The value of loop gain at which oscillation occurs is about the same for both circuits.

Unfortunately the frequency characteristic of a cascode bridged-T resembles more an inverted V than a narrow rectangle. However if three cascode bridged-T's are cascaded to form a "flat-staggered-triple"<sup>(19)</sup>, a much closer approximation to a rectangular spectrum can be obtained. The flat-staggered-triple has the three mid-band frequencies displaced slightly, resulting in a characteristic having a reasonably flat top and sharply sloping sides. (See Fig. 22)

The output circuit provides about 50 volts for input to Unit II. It was found necessary to load the final cascode bridged-T with a cathode follower; Miller-effect capacitance in the 6SL7 triode caused oscillation in the bridged-T circuit.

Fig. 8 shows the clippers, the phase inverter, and a noise-voltage meter. The signal is clipped five times and amplified twice; the diodes clip three times, and the input circuit to each pentode acts as a clipper by effectively

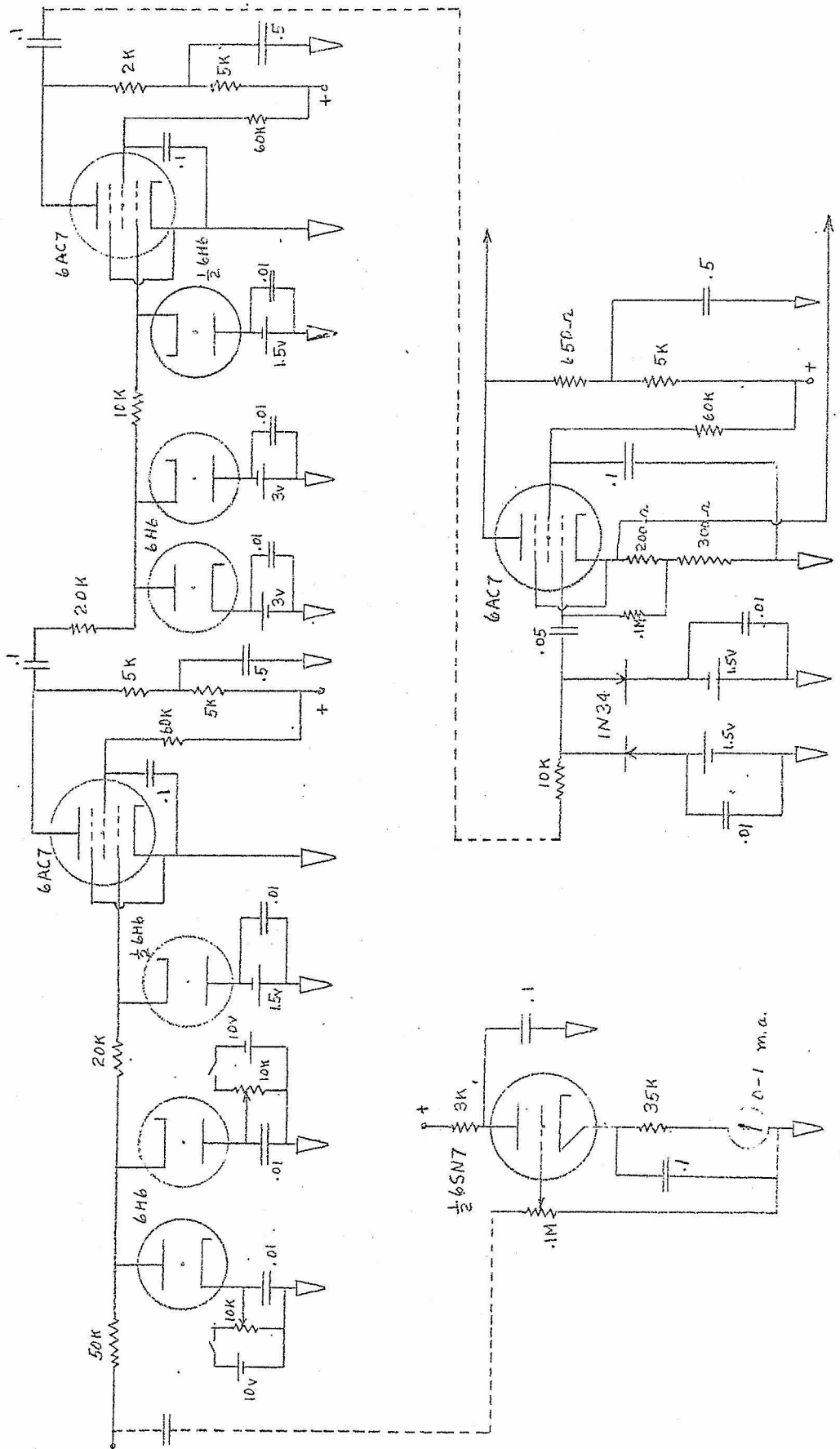


Fig. 3. Clippers, noise-current meter, and phase inverter.

shortening the grid base to about one volt. Actually fewer stages could have been used, since the rise time is limited by the integrating action of the line resistor and the diode capacitance. For this reason a pair of 1N34 crystal diodes is the final clipper; their capacitance is less than that of a 6H6 by a factor of four.

The variable biasing arrangement on the first pair of diodes is included to ensure that the zero spacings are not distorted; the pentodes give different slopes to the positive and negative rises of the square wave, because the transconductance varies with grid voltage. This adjustment was found to be quite critical in affecting the final output.

The phase inverter is orthodox. The plate half of the circuit reacted violently to noise and ripple in the plate supply, and a well regulated power supply was absolutely necessary. A higher total gain would have lessened the effect of noise and ripple, although at the expense of rise time.

In Fig. 9 we have the differentiators, clippers, mixer, and Unit II output circuit. The two-tube mixer was thought necessary for isolation purposes. Matching in the output coaxial-cable circuit was not critical, although an attempt was made to match at both ends of the line.

The next figure, Fig. 10, shows the input circuit and first multivibrator of Unit III. The function of the multivibrator is to shape the incoming pulses. The first amplifier inverts the positive pulses from Unit II to give the

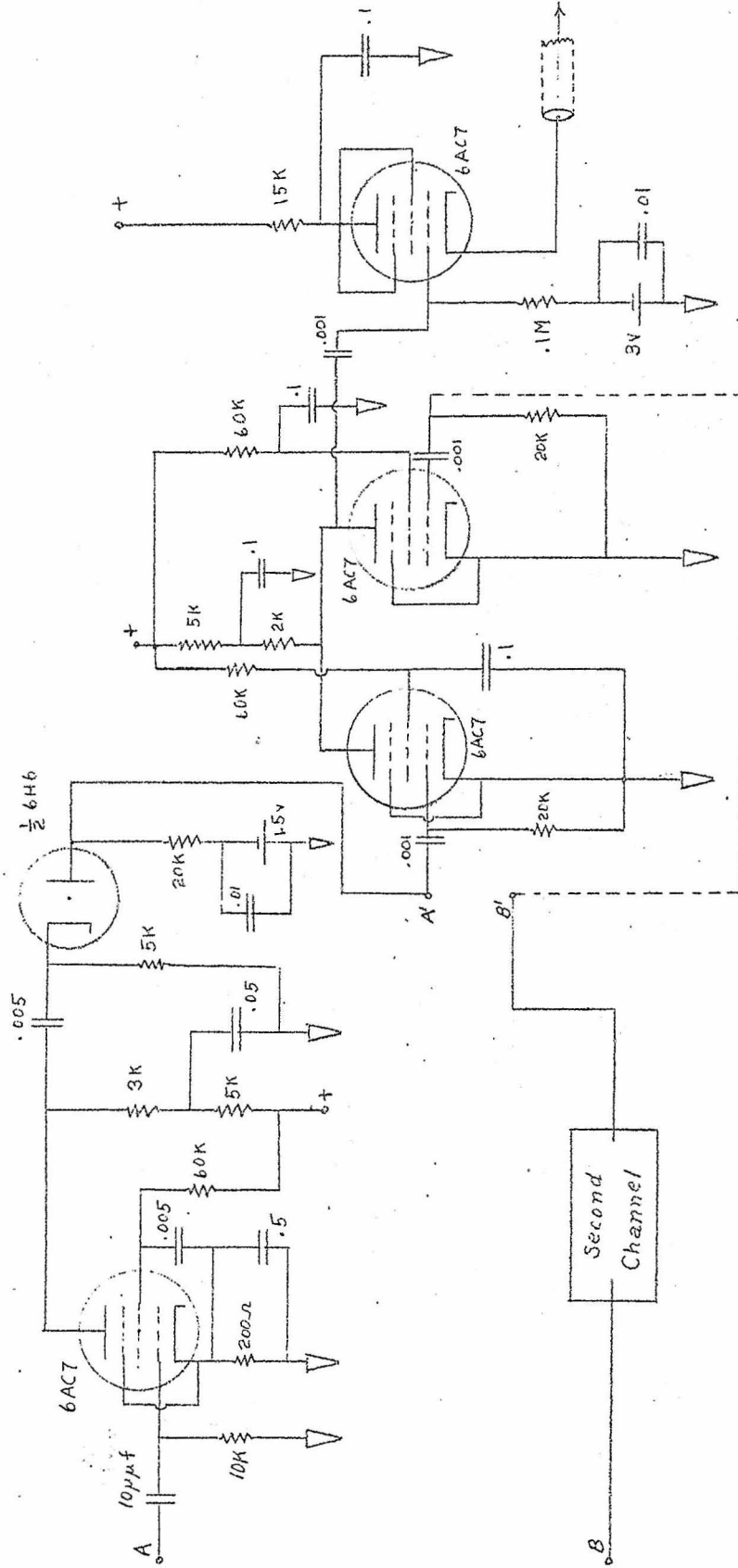


Fig. 9. Differentiators, mixer, and output circuit.

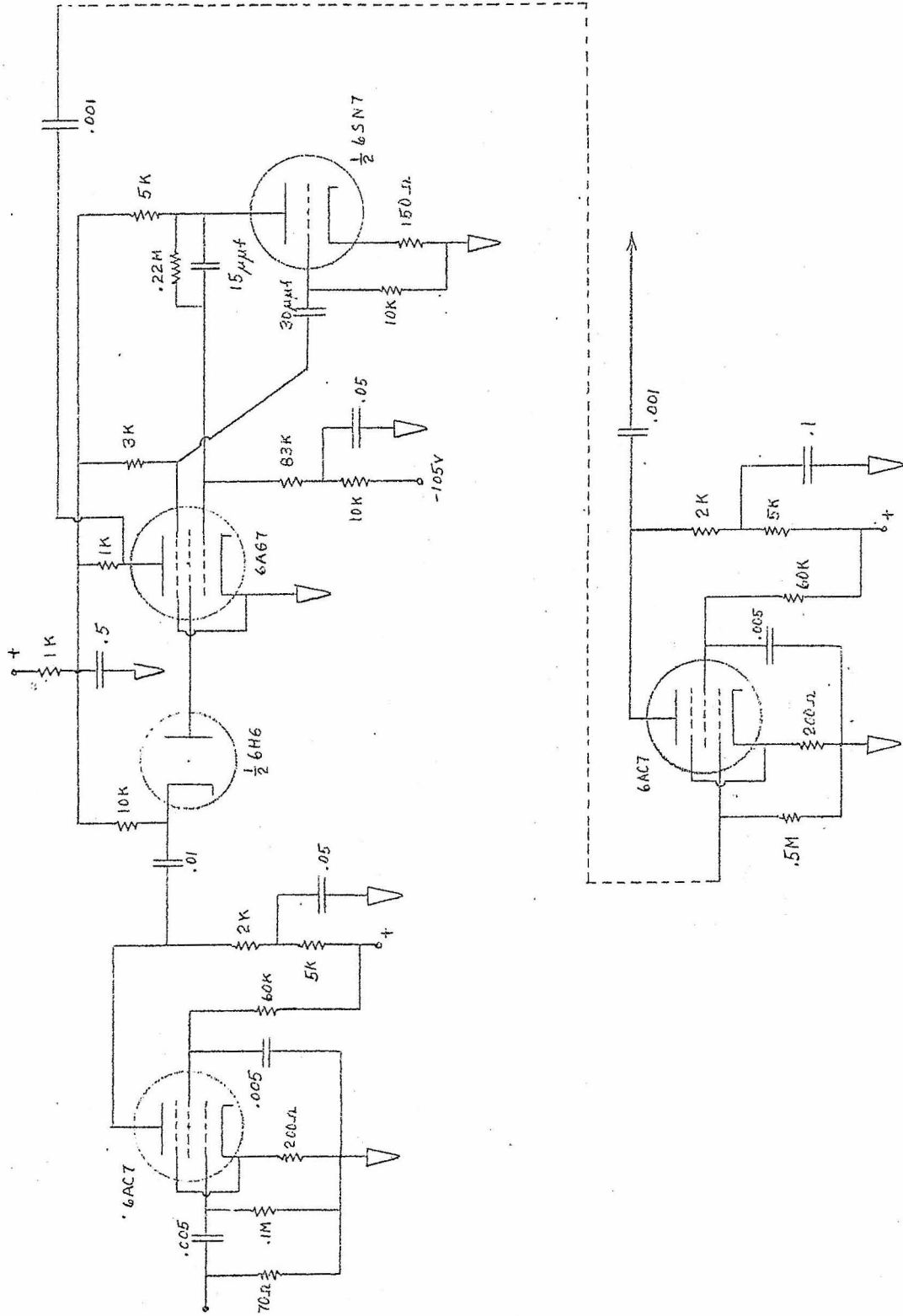


Fig. 10. Inverter amplifiers and first multivibrator.

negative pulses required to trigger the multivibrator. About (-)5 volts is required for triggering, and output pulses are (-)30 volts. Pulse width is approximately one micro-second.

The sawtooth timing waveform generator, the clipper, and the differentiator are illustrated in Fig. 11. The sawtooth generator operates by charging a resistance-capacitance combination; each successive pulse discharges the condenser through the parallel triodes. A diode "restorer" assures that each segment of the sawtooth starts at the same voltage. Several other sawtooth generators were tested; the next best was the Miller Integrator.<sup>(19)</sup> This circuit employs capacitive feedback around a DC amplifier, and was found to have superior linearity; however persistent overshoots at the beginning of each segment made it less satisfactory. The linearity deviation of the circuit shown, expressed as deviation of the curve from a straight line, was less than 0.5%.

The sawtooth generator is coupled through a cathode follower to the clipper. The clipping voltage level is determined by the 10K potentiometer setting, while the voltage difference between the extreme settings is a function of the resistance paralleled with the potentiometer. The voltage range is adjusted by means of the 30K potentiometers; ganging them makes the voltage difference between clipping limits independent of their setting, which makes for simplified calibration.

The clipper feeds a differentiator and pulse ampli-

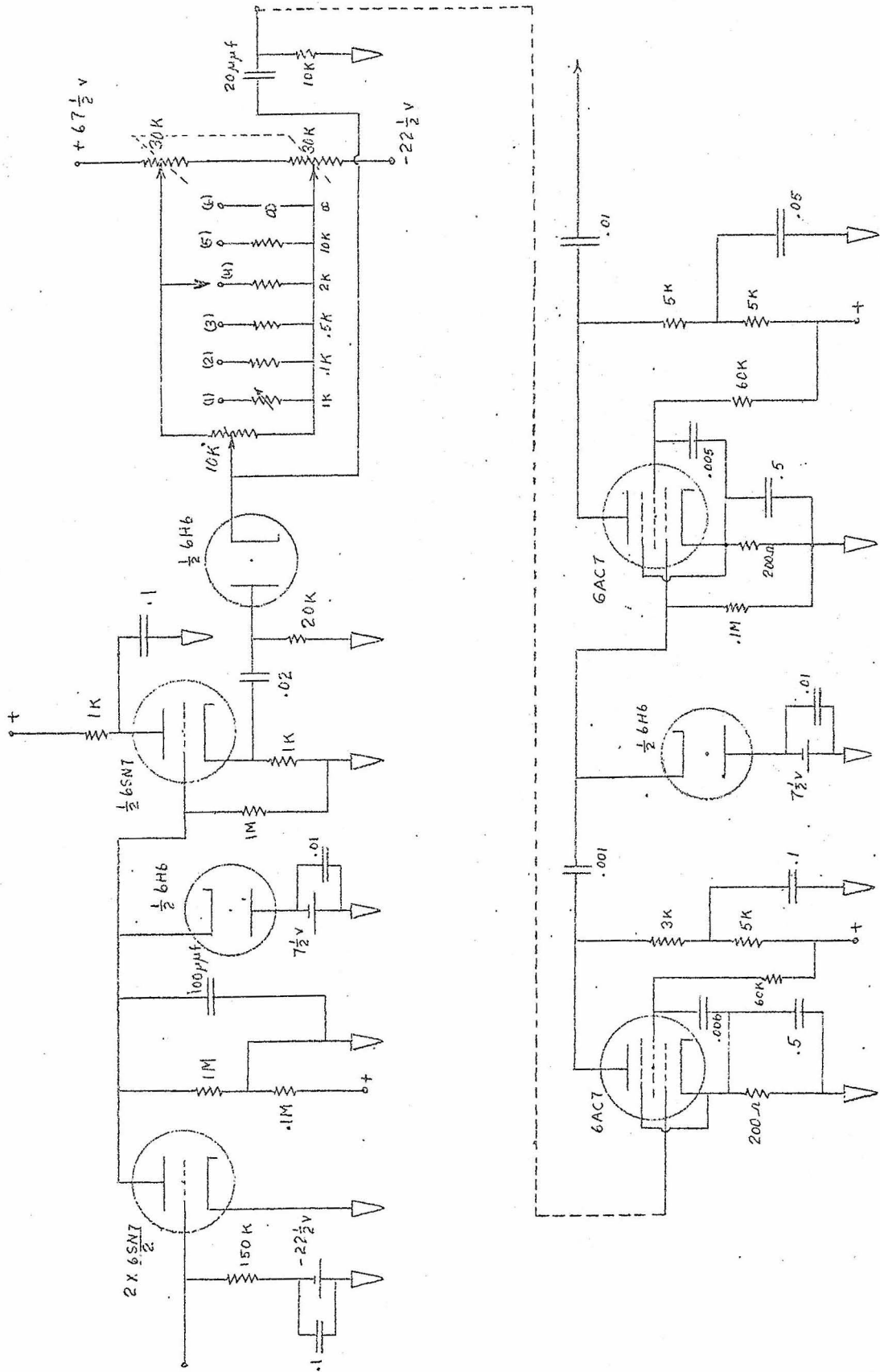


Fig. 11. Sawtooth generator, clipper, and differentiator.

fiers. The diode between amplifier stages removes the unwanted transients generated during the slanting portion of the sawtooth wave.

Fig. 12 gives the second multivibrator and the final output circuit. The second multivibrator is identical with the first, except that the pulse length is greater.

The output circuit has some features of interest. Its function is to obtain a number proportional to the number of pulses delivered to it. This is done by integrating the pulses through the charging of a condenser-resistor combination. To measure the condenser voltage a triode and two voltage-regulator tubes are used. The 20K potentiometer is set such that when no pulses are delivered the meter current is zero. But when the condenser is charged, its voltage appears at the grid of the triode, and a current unbalance results; thus we obtain a meter reading which is a function of the number of pulses applied to the pentode.

Four power supplies were used in conjunction with the equipment described above. Three were plate supplies capable of delivering 200 milliamperes at 300 volts, and the fourth supplied the -105 volt bias for the multivibrators. Two of the plate supplies, those for units II and III, were electronically regulated; the plate supply for Unit I had especially heavy filtering. The -105 volt bias was taken from a VR-105 voltage-regulator tube. Power-supply ripple and noise affected markedly the performance of the system by appearing in the output-meter reading.

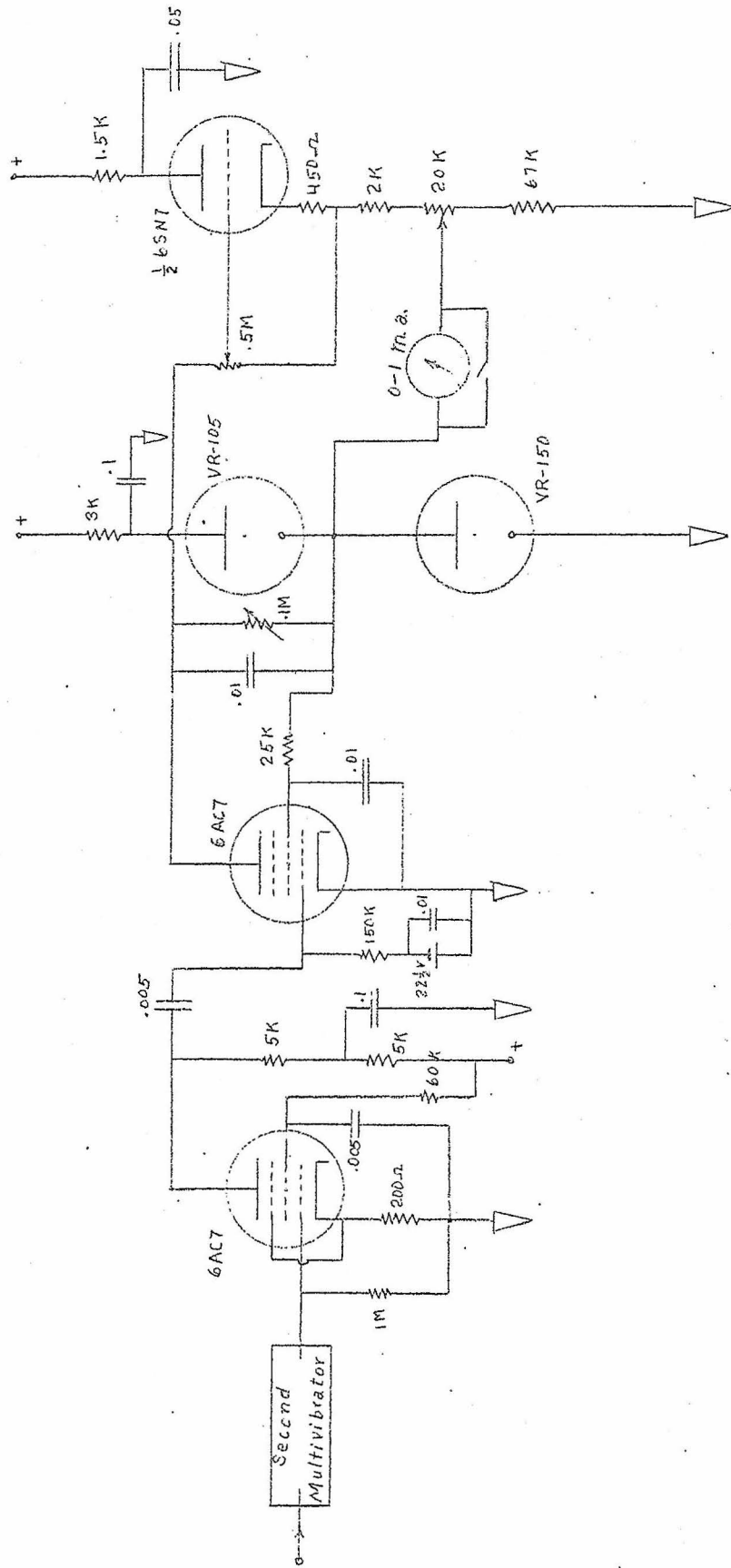


Fig. 12. Second multivibrator and output meter.

In order to illustrate the operation of the apparatus, photographs of several oscilloscope traces have been included. For these traces a 20 KC signal was used. In Fig. 13 we have the clipped signal at the 1N34 diodes. Fig. 14 gives the first multivibrator output, and Fig. 15 shows the sawtooth timing waveform. Fig. 16 shows the second multivibrator output. A trace of heavily filtered random noise is shown in Fig. 17. The noise is obtained by passing noise from the thyratron through the flat-staggered-triple filter. Note its resemblance to a sinusoid.

Calibration. To interpret the output meter reading properly we must know two things: first, the number of zeros per second that the meter reading represents, and second, the smallest zero-crossing period being counted by the meter. To determine the first quantity we may by-pass the sawtooth wave clipping circuit and record the output meter reading as a function of the input frequency, using a sinusoidal input. Then twice the frequency gives the number of zeros per second. This curve is given in Fig. 18; the values of the number of zeros per second have been expressed as a fraction of 50,000, which is the number of zeros per second corresponding to full-scale meter deflection. This quantity is later used as the distribution function. The linear character of this curve was useful since, with reasonable accuracy, the meter reading can be plotted directly on the distribution function curve.

To determine the clipping level of the sawtooth timing

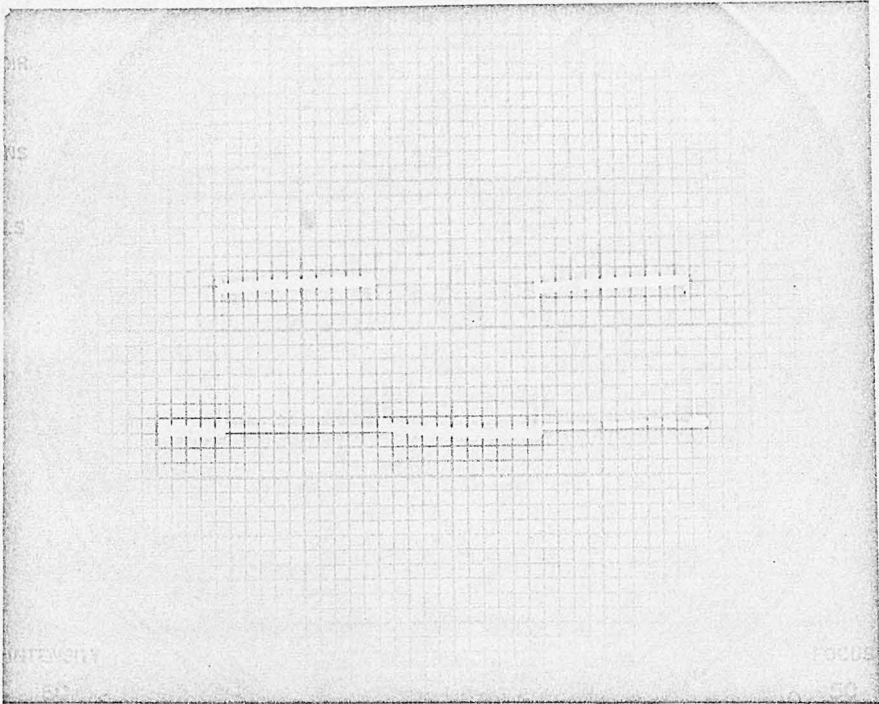


Fig. 13. Clipped signal.

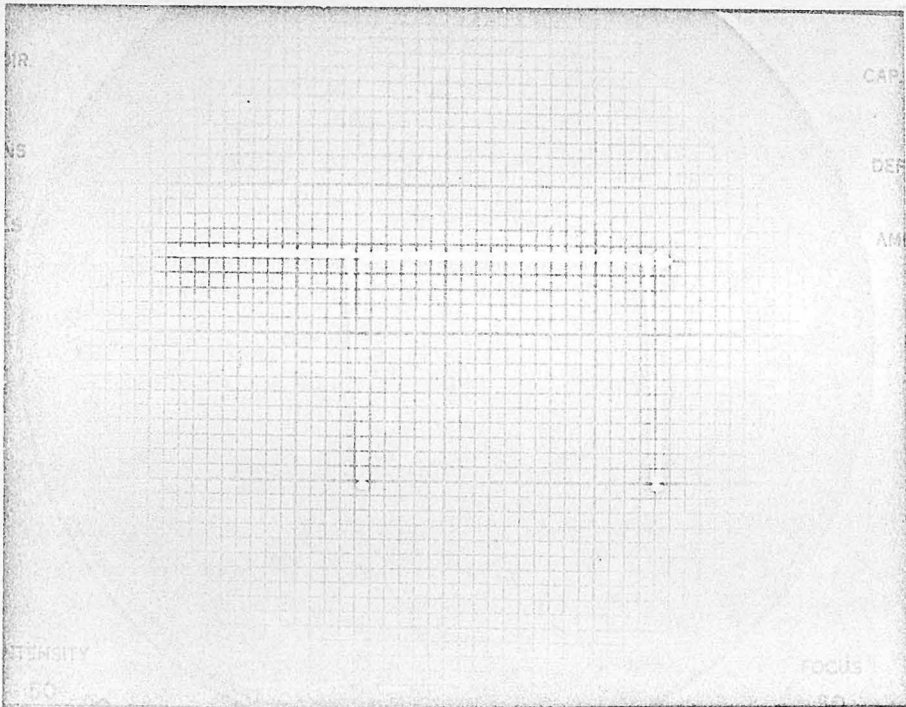


Fig. 14. First multivibrator output.

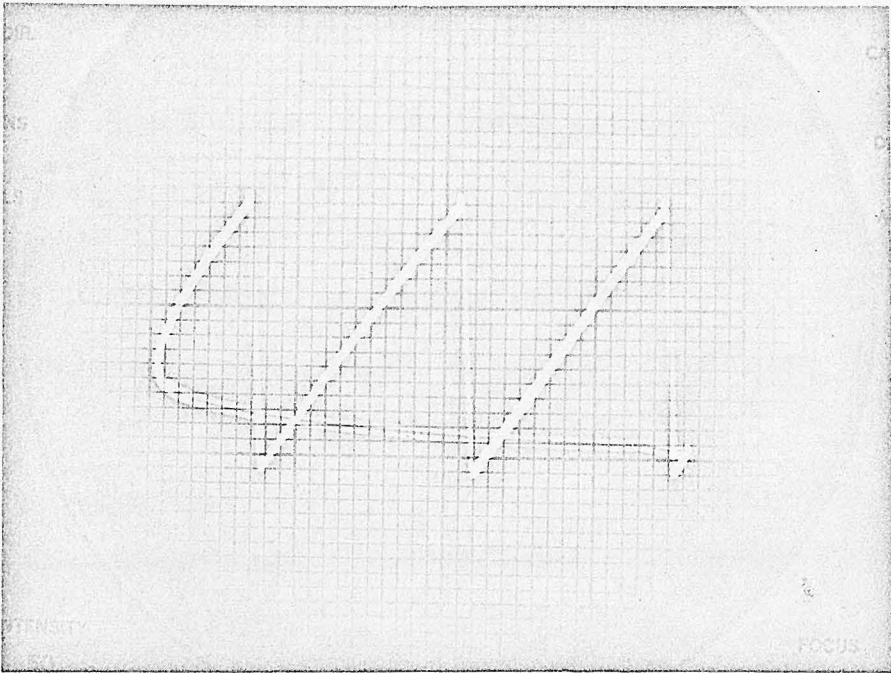


Fig. 15. Sawtooth timing waveform.

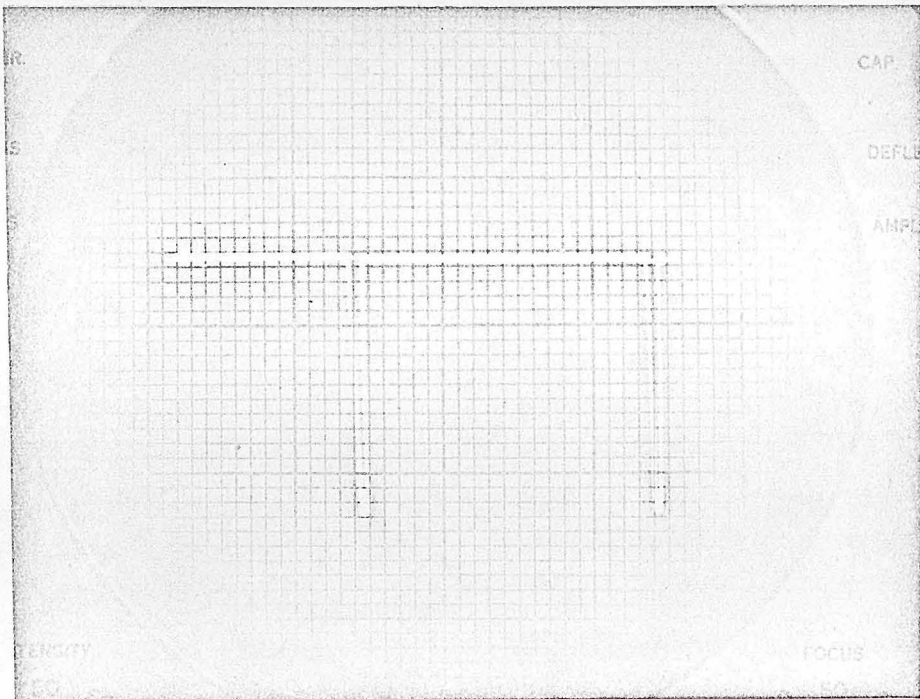


Fig. 16. Second multivibrator output.

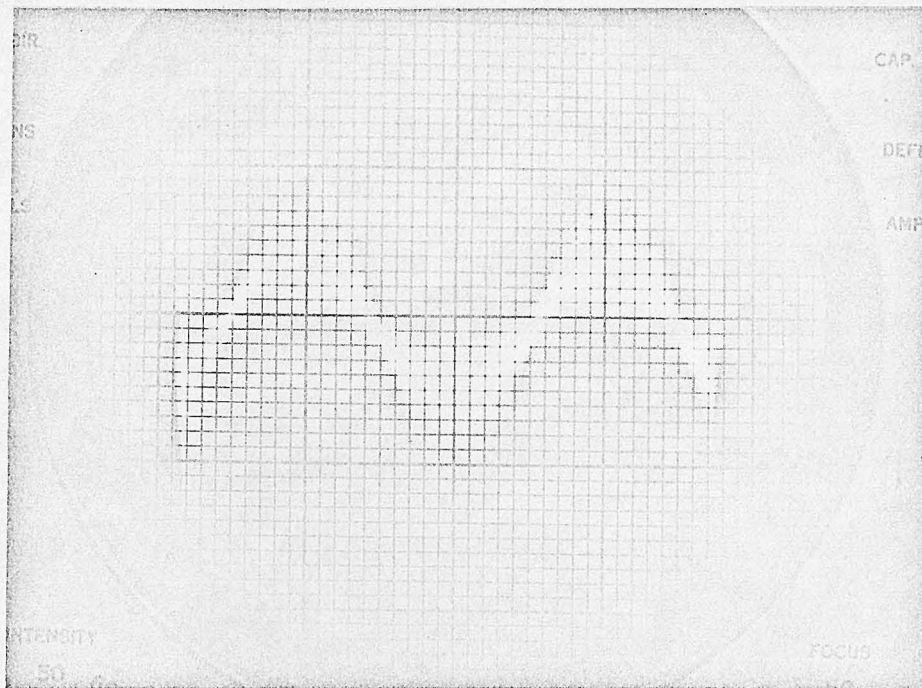


Fig. 17. Heavily filtered random noise.

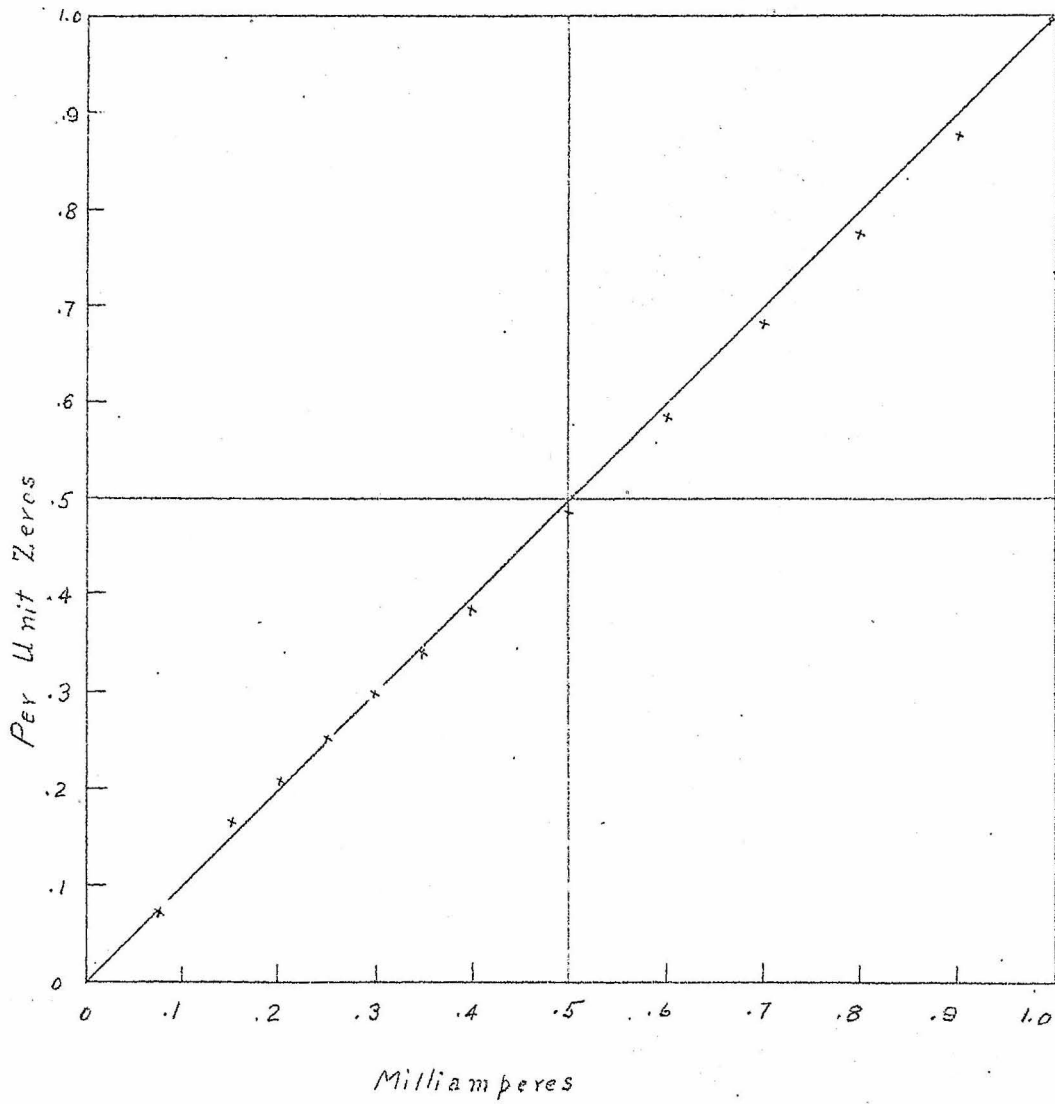


Fig. 18. Meter Calibration.

waveform in time units we may set the 10K potentiometer in the clipper at a given value and find at what input frequency the meter deflects. The time clipping level is then one-half the period, or  $1/2f$ . Curves obtained in this way are shown in Fig. 19 and Fig. 20. The abscissae are units on the 10K potentiometer dial (0-100), and the R-numbers indicate the resistance being paralleled with the potentiometer.

Figures 21, 22, and 23 show the frequency response of several combinations of the bridged-T filters. In Fig. 23 resistance has been added in several steps to the inductance of the bridged-T. To obtain the ohmic resistance from the figures shown, multiply by 100. Since the range of frequencies in the pass-band of these filters is small, a heterodyning unit was constructed which compared the unknown frequency with a fixed standard.

Photographs of Equipment. Figures 24-28 inclusive show the experimental system. Fig. 24 shows all of the components; in the foreground we see Units I, II, and III, and in the rear left and right the power supplies are shown. The small chassis on top of the large power supply is the -105 volt multivibrator supply.

Errors and Limitations. It is difficult to assign a figure of accuracy to the measurements made by this system. An educated guess would place the figure near five per cent. The principal source of error was extraneous noise originating in the power supplies. To eliminate this noise it would have been necessary to replace two power supplies, and

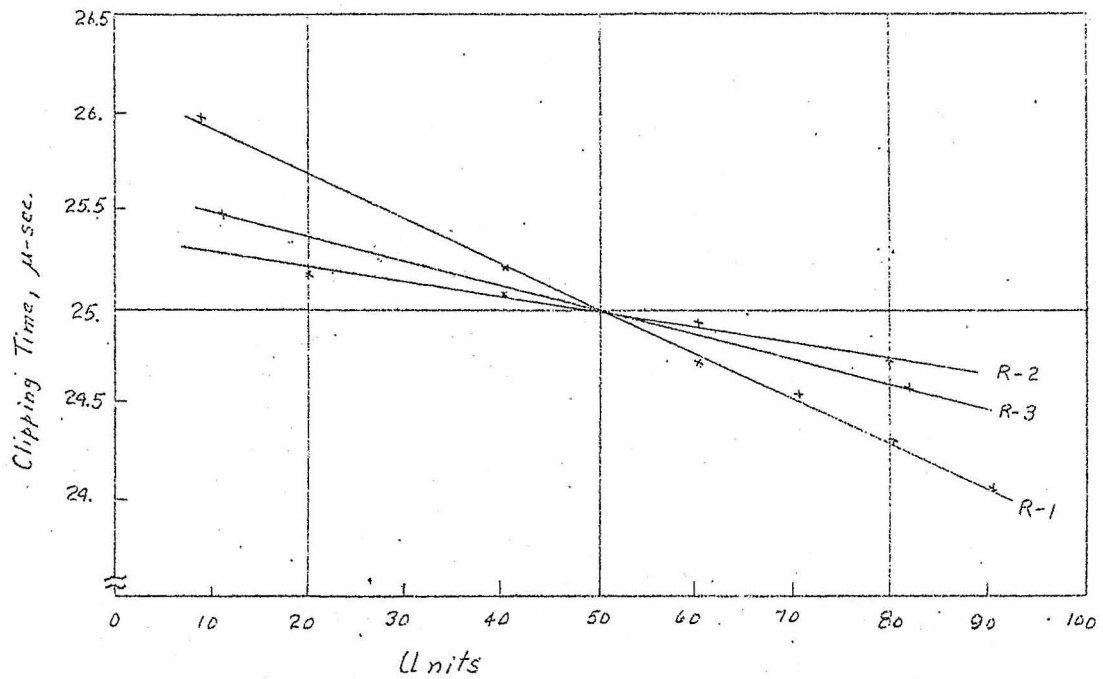


Fig. 19. Clipping Time, Ranges 1, 2 and 3.

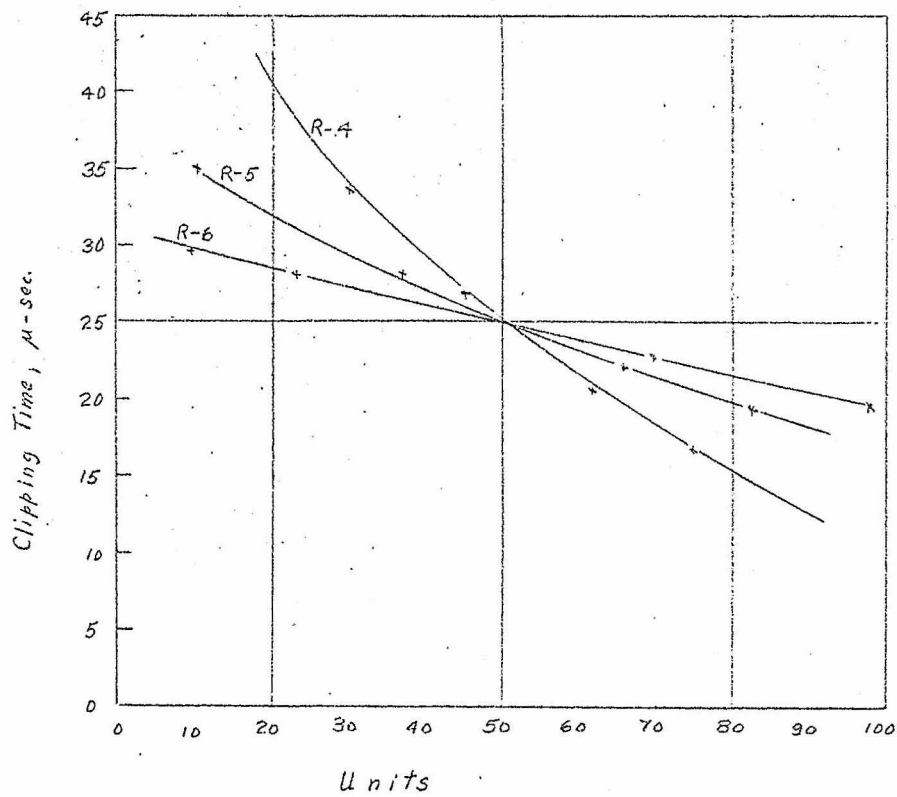


Fig. 20. Clipping Time, Ranges 4, 5, and 6.

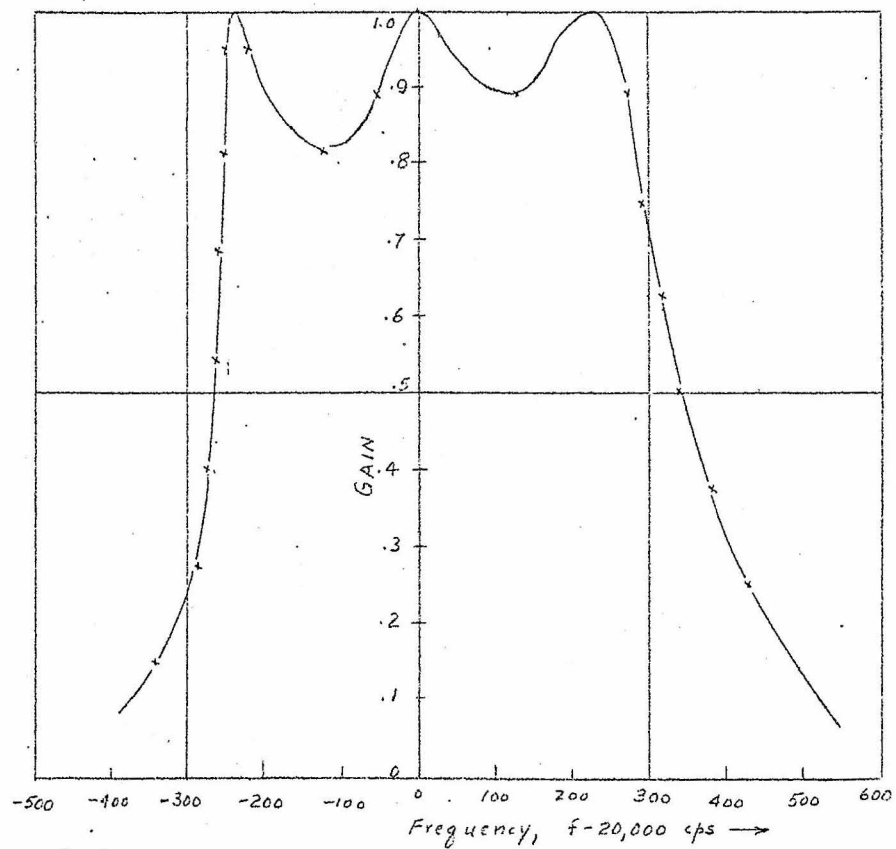
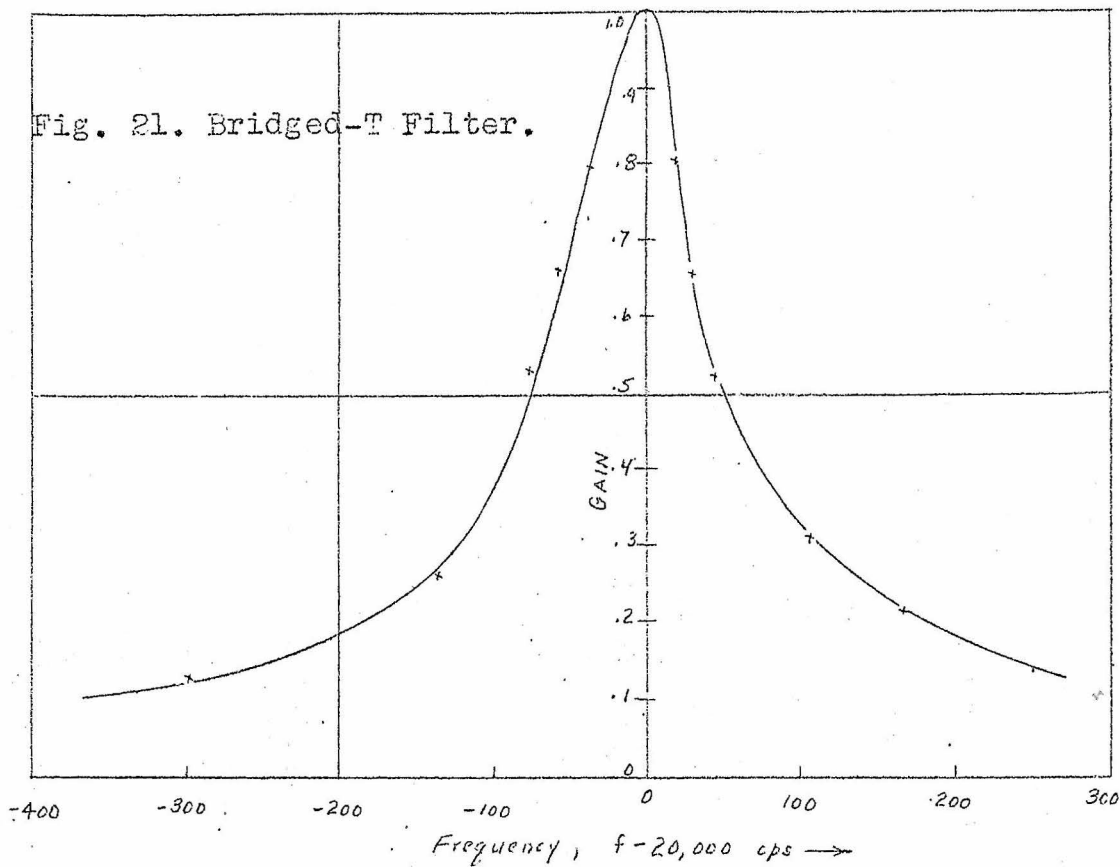


Fig. 22. Flat-staggered-triple Filter.

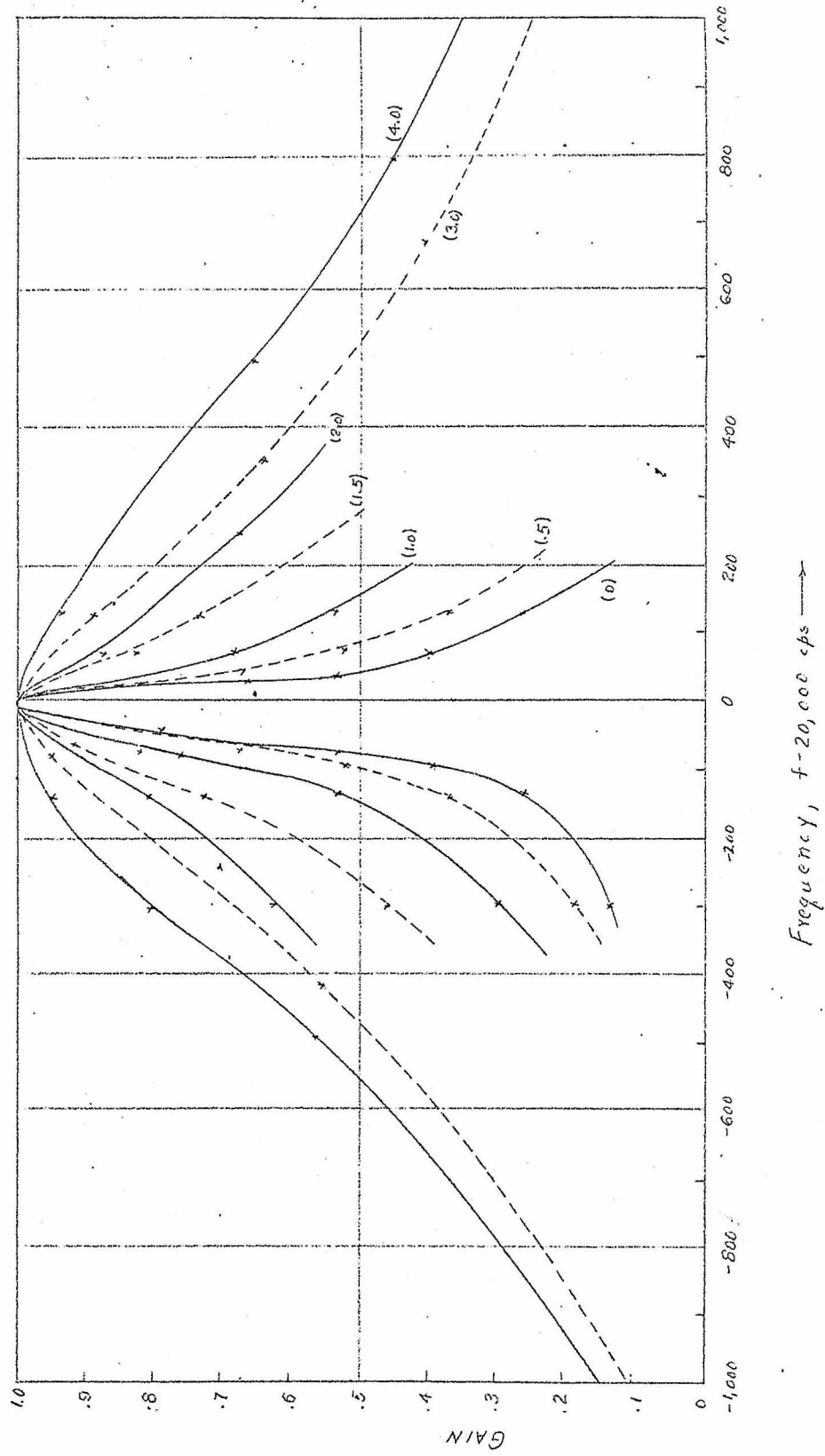


Fig. 23. Frequency response of bridged-T filters.

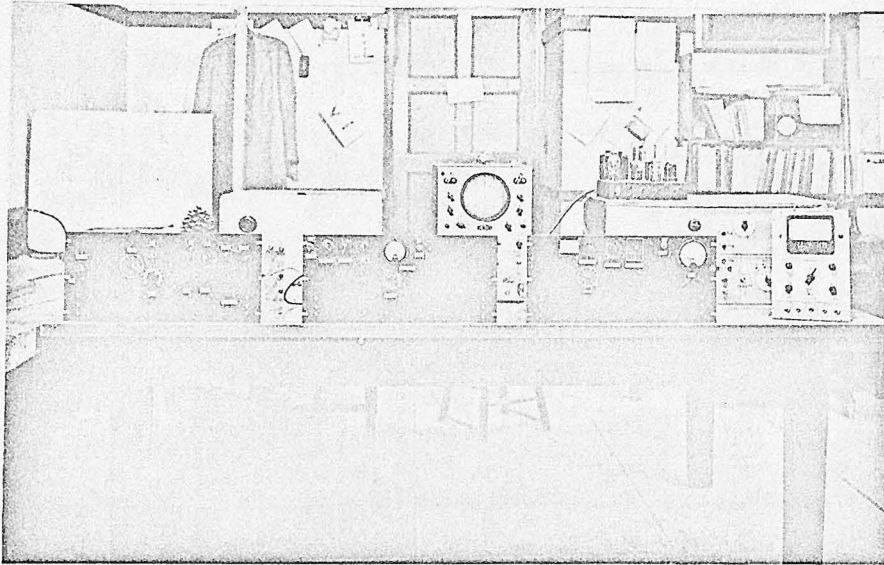


Fig. 24. Complete experimental apparatus.

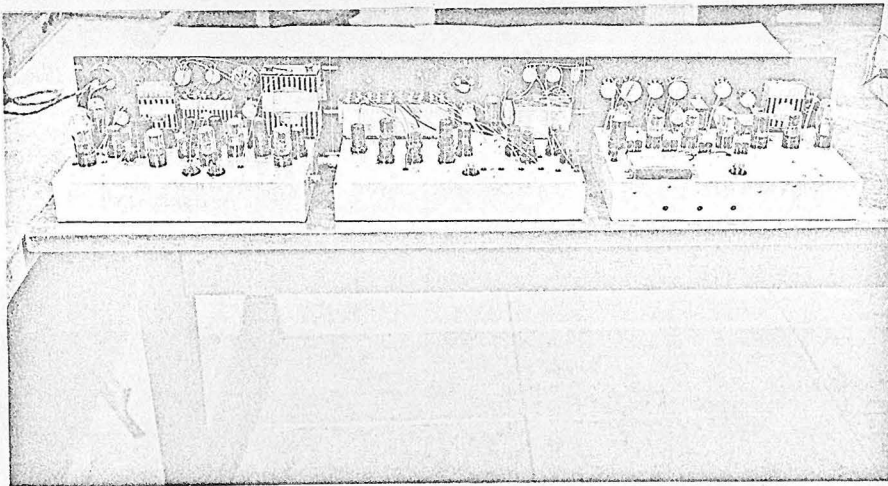


Fig. 25. Units I, II, and III, rear view.

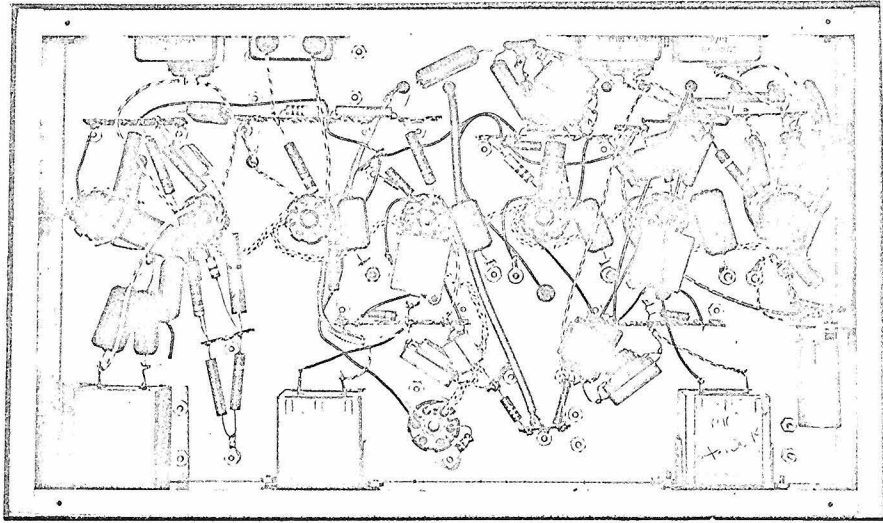


Fig. 26. Unit I, bottom view.

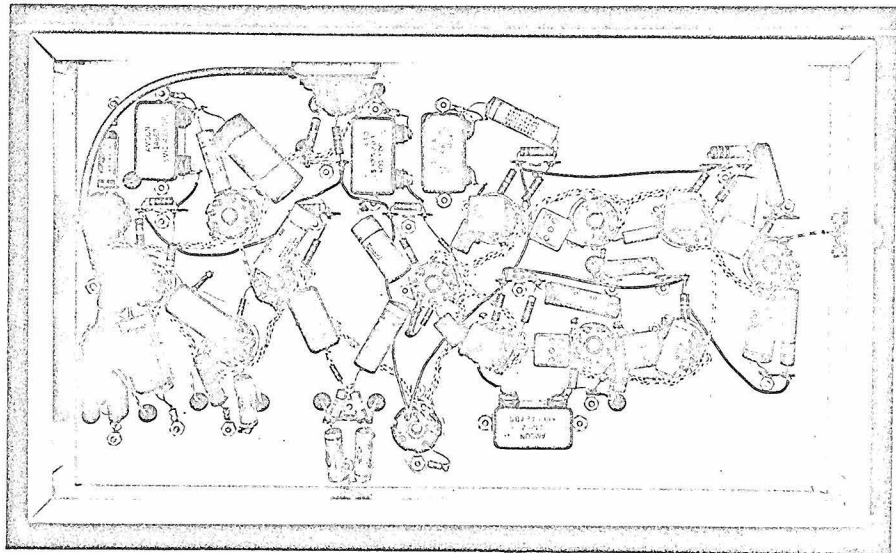


Fig. 27. Unit II, bottom view.

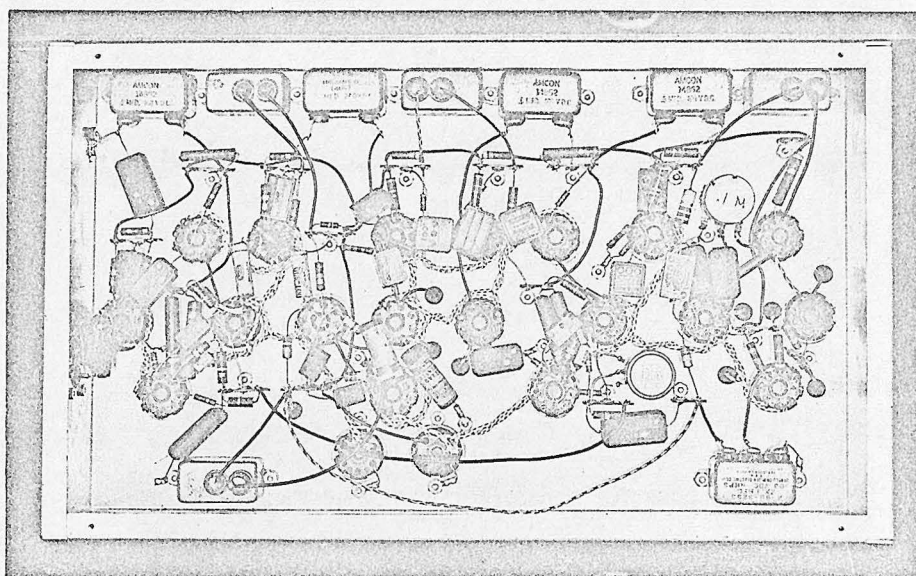


Fig. 28. Unit III, bottom view.

also to use batteries for plate and filament in the noise generator and the early amplifier stages.

## IV. EXPERIMENTAL RESULTS

To obtain the distribution function corresponding to a given filter it is necessary only to record the output meter current as a function of the clipping potentiometer setting; entering the calibration curves with these values gives the distribution function directly. The frequency function can be obtained from the distribution function by graphical differentiation. Each curve of meter current versus potentiometer setting was taken several times, and a mean used, since noise caused some fluctuation in the readings.

It is more realistic and convenient to present the experimental data on a micro-second time base than to use the dimensionless  $\alpha$  of Section II. We need, therefore, the theoretical distributions on a micro-second base. For a mid-band frequency of 20 KC we have

$$p_0'(\tau) = \frac{6.93 Q}{(10^4 + 192 Q^2 \tau^2)^{\frac{3}{2}}} \quad (11)$$

where  $\delta\tau = |\tau - 25|$

and the prime indicates that the time base is in micro-seconds. The distribution function is found by integrating the above expression. It is given by

$$D_0'(\tau) = \frac{1}{2} \pm \frac{6.98 (Q \delta\tau)}{[10^4 + 192 (Q \delta\tau)^2]^{\frac{1}{2}}} \quad (12)$$

Note that the distribution functions given by Eq. 12 differ, for various  $Q$ 's, only by a scale constant on the time base.

Fig. 29 shows the distribution function obtained experimentally from the flat-staggered-triple (FST) filter of Fig. 22, together with a theoretical distribution function which approximates it. The accompanying frequency functions are shown in Fig. 30. The asymmetry of the measured curves is probably due to the asymmetry in the frequency response of the filter, notably that caused by the difference in the slopes of the sides of the characteristic. To correlate the distribution function with the spectrum we compare the equivalent  $Q$  of the filter, given by Eq. 10, with the  $Q$  corresponding to the measured distribution function. Proceeding according to Eq. 10 for the case of  $n=2$  we have, approximately,

$$Q_1 = 34.5 \quad (-260 < \Delta f < 320)$$

$$Q_2 = 20 \quad (-450 < \Delta f < 500)$$

$$A_1' = 1$$

$$A_2' = .2$$

$$h = .113$$

$$Q_e = .942 Q_1 = 32.4$$

(Note that the spectrum is proportional to the square of the amplitude of the frequency response.) Thus for the FST filter an examination of the frequency response gives us

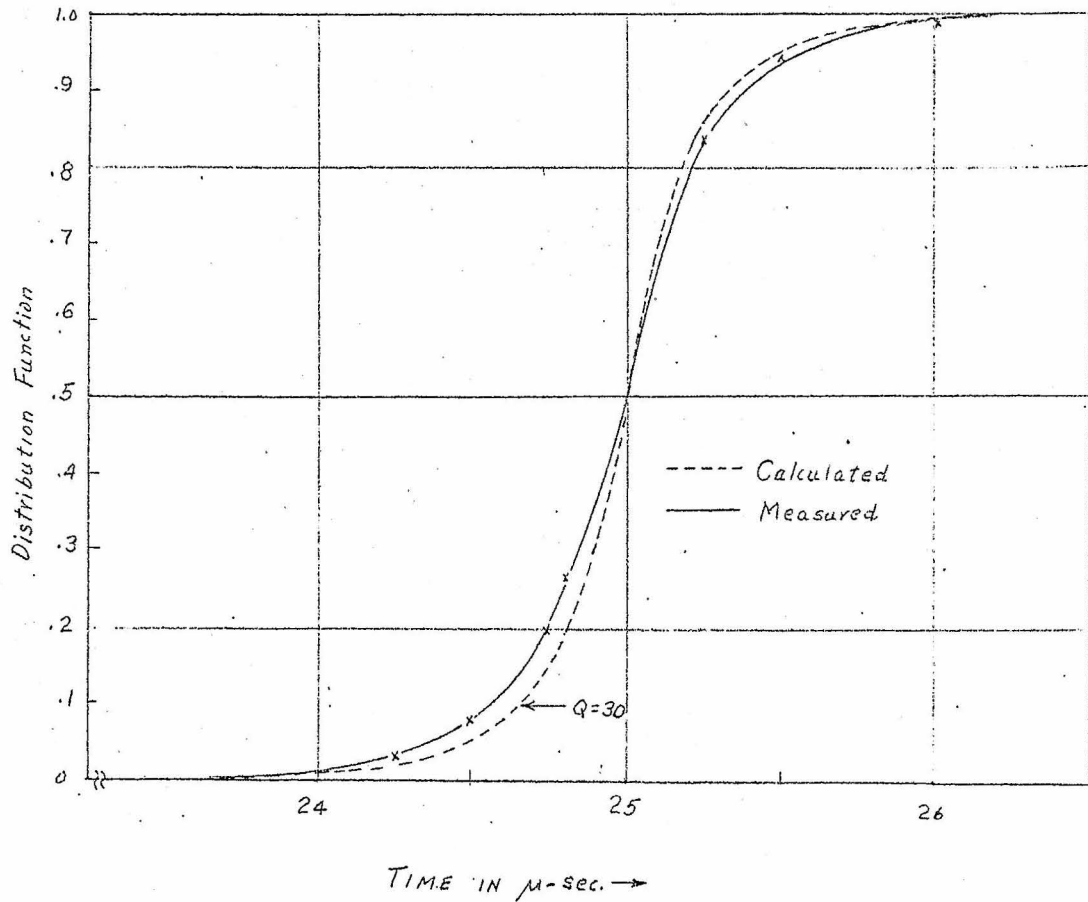


Fig. 29. Distribution function, flat-staggered-triple filter.

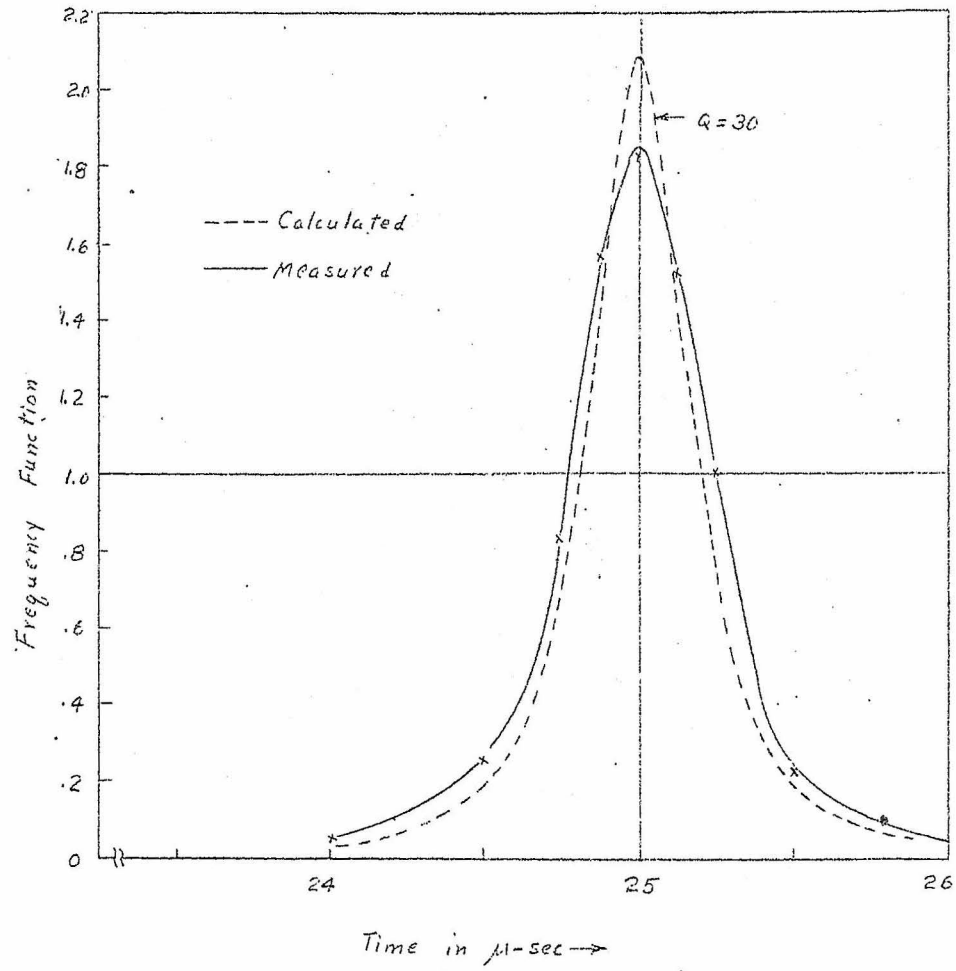


Fig. 30. Frequency function, flat-staggered-triple filter.

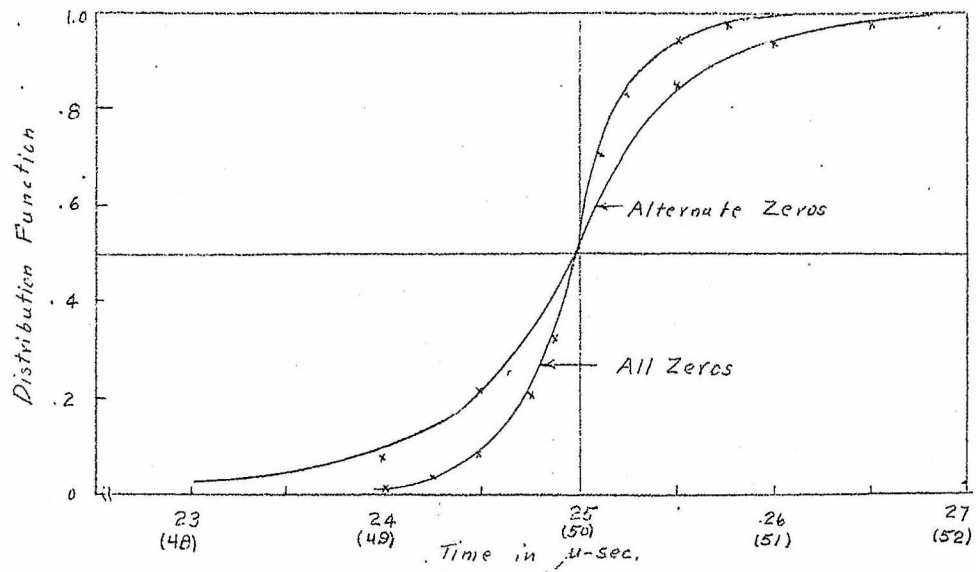
an equivalent  $Q$  of 32.4, while the distribution function indicates a  $Q$  of about 30. This degree of correspondence between  $Q$ 's, as well as between the shapes of measured and predicted probability functions, is considered good by the author.

The expression analogous to Eq. 8 for any  $n$  is

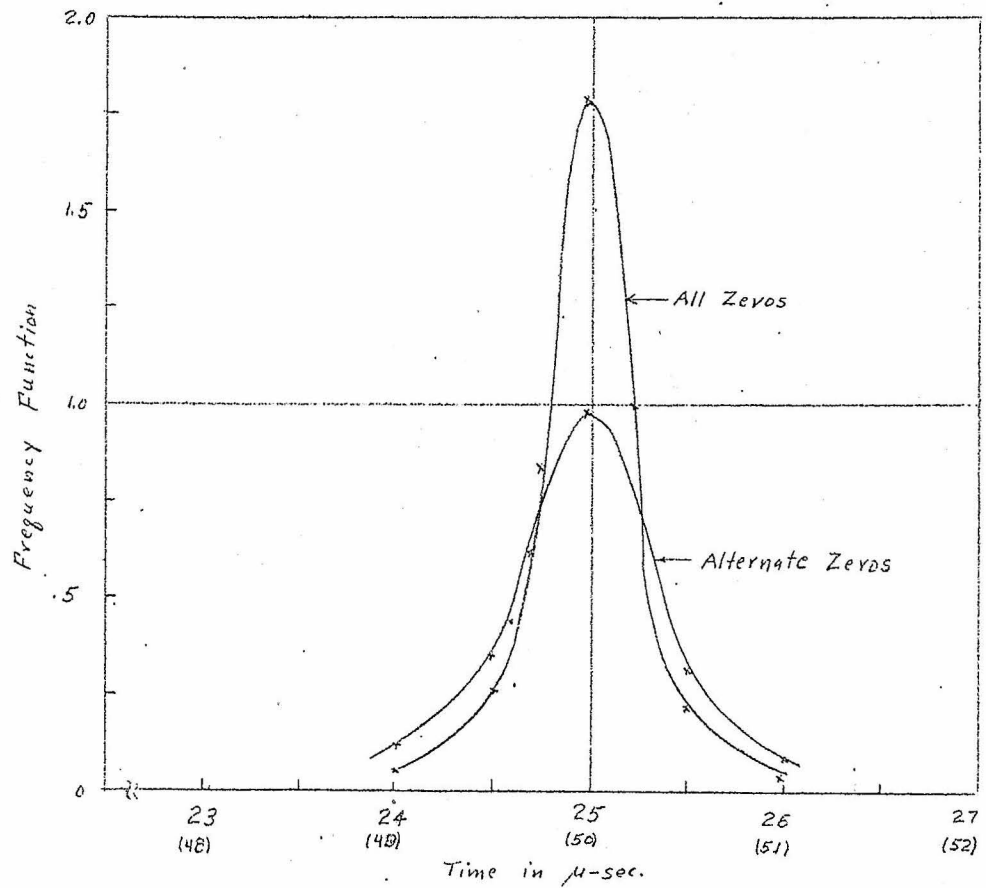
$$f_0(\alpha) = \frac{n^2 \pi^2}{12Q^2 \left[ \frac{n^2 \pi^2}{12Q^2} + 4\left(\alpha - \frac{n\pi}{2}\right)^2 \right]^{\frac{3}{2}}}$$

Thus the frequency function about two half-periods ( $n=2$ ) behaves as if its  $Q$  were halved. To check this experimentally a run was made with one of the inverting channels dead; this meant that only alternate zeros were considered. The results are shown in Fig. 31. The ratio of the  $Q$ 's for the curves shown is very nearly two.

The next sequence of curves, Figures 32-35 inclusive, shows distribution functions from a single bridged-T (BT) filter. The numbers in parentheses indicate the resistance added to the inductance arm of the bridged-T. The  $Q$  indicated is that of the theoretical curve accompanying the measured one. (See Fig. 23 for the filter characteristics.) The frequency range of these filters violates the assumptions of our theory; we no longer have  $Q \gg 1$  and  $|\alpha - \frac{n\pi}{2}| \ll 1$ . Some agreement between theory and experiment can be obtained from BT(0), the sharpest characteristic. Proceeding according to Eq. 10 we have, roughly,

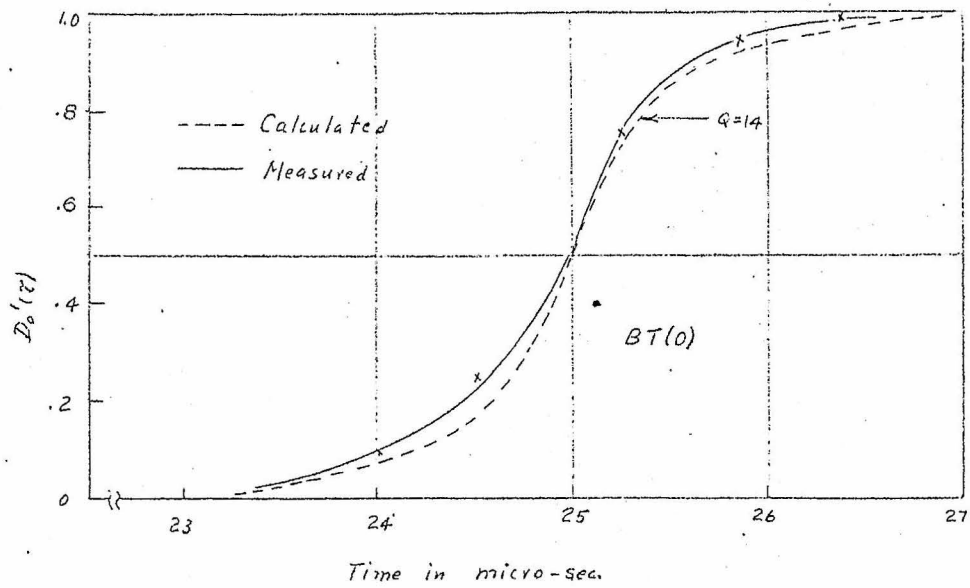


(a). Distribution function.

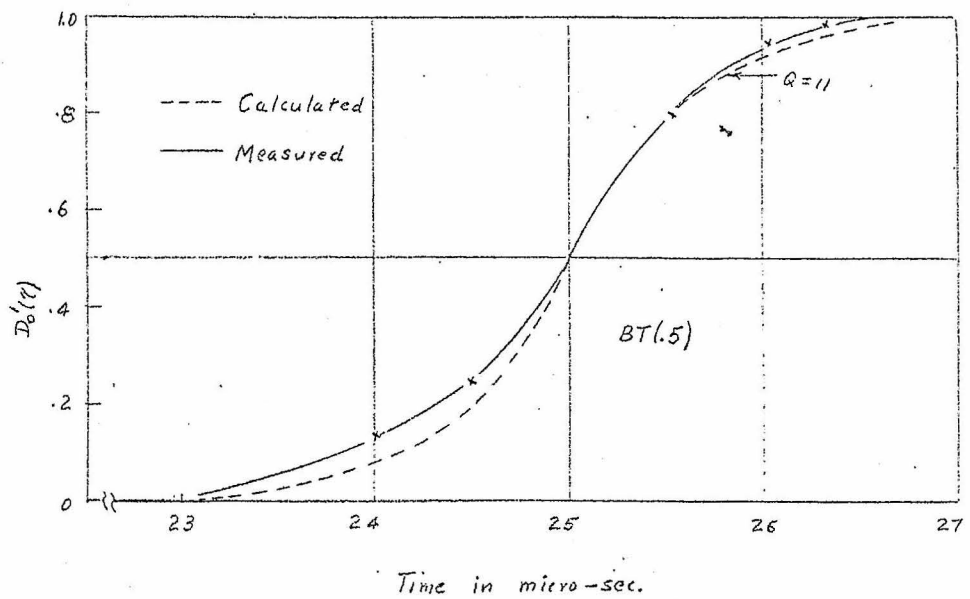


(b). Frequency function.

Fig. 31. All and one-half the zeros, flat-staggered-triple filter.

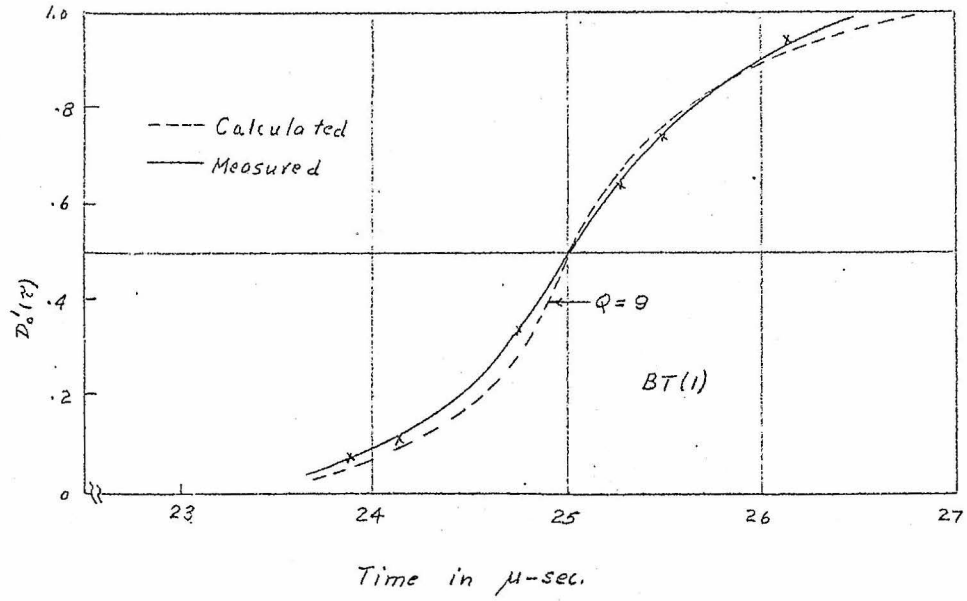


(a). BT(0)

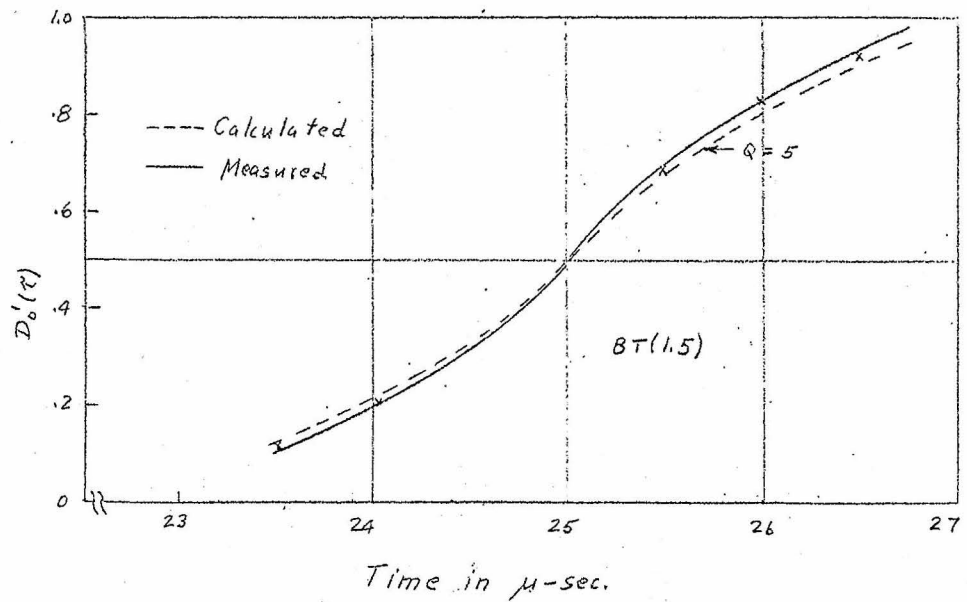


(b). BT(.5)

Fig. 32. Distribution functions for bridged-T filters BT(0) and BT(.5).

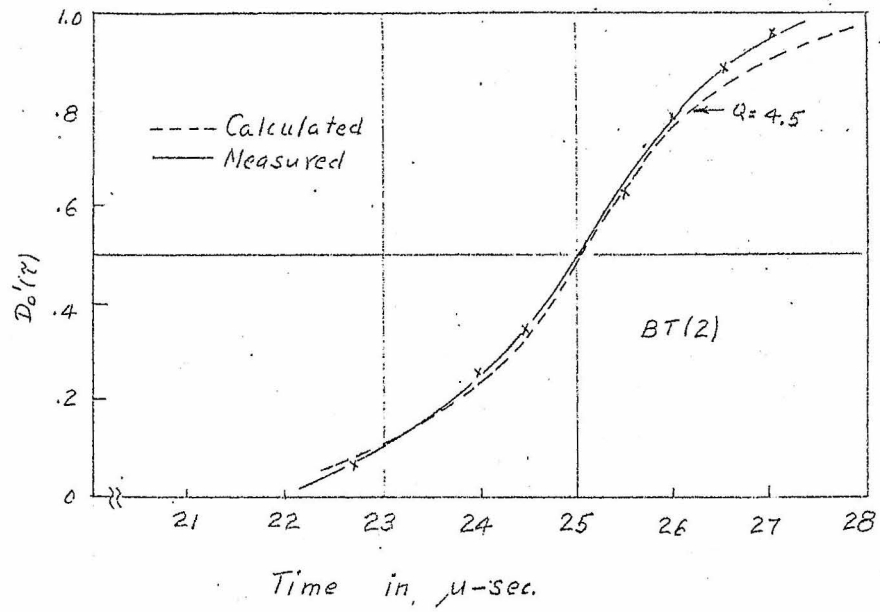


(a). BT(1).

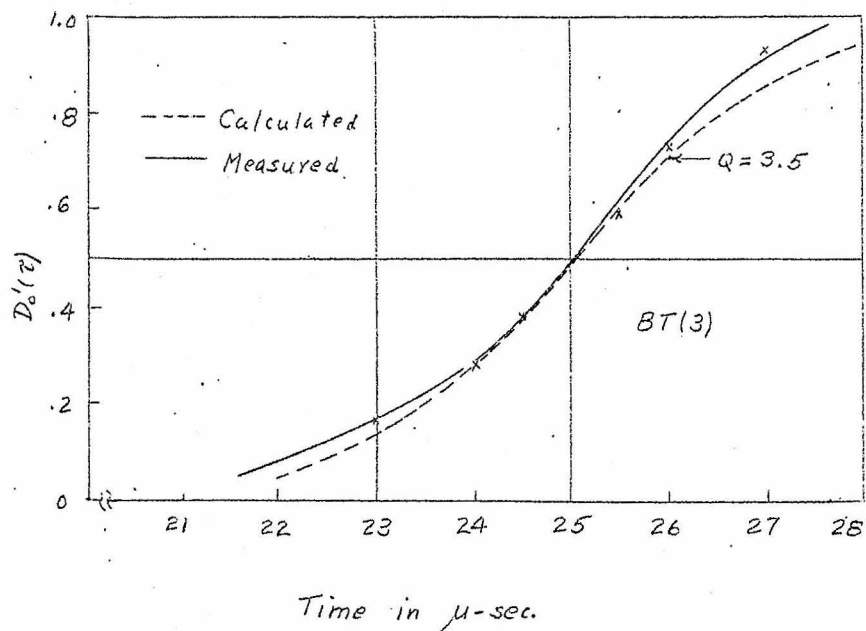


(b). BT(1.5).

Fig. 33. Distribution functions for bridged-T filters BT(1) and BT(1.5).



(a). BT(2).



(b). BT(3).

Fig. 34. Distribution functions for bridged-T filters BT(2) and BT(3).

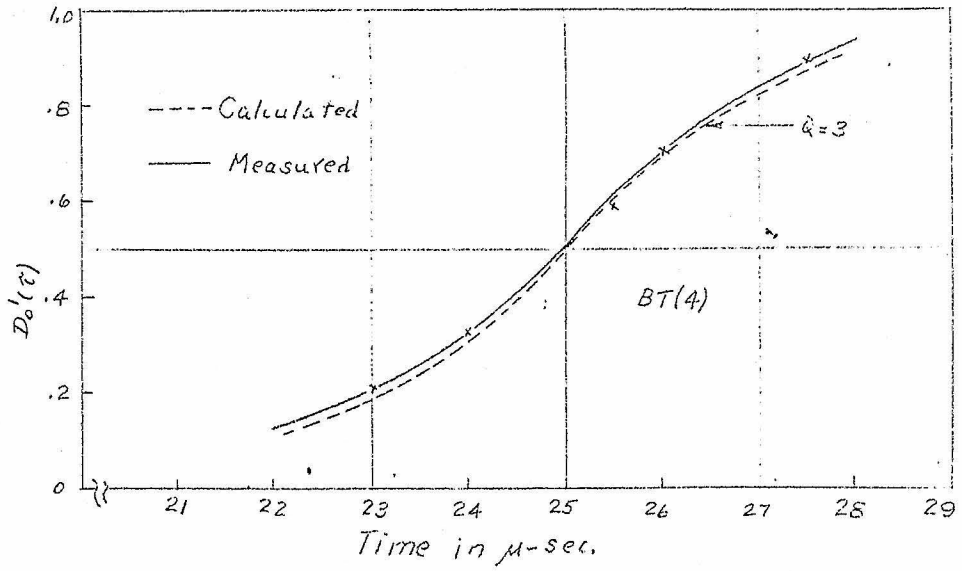


Fig. 35. Distribution function for bridged-T filter BT(4).

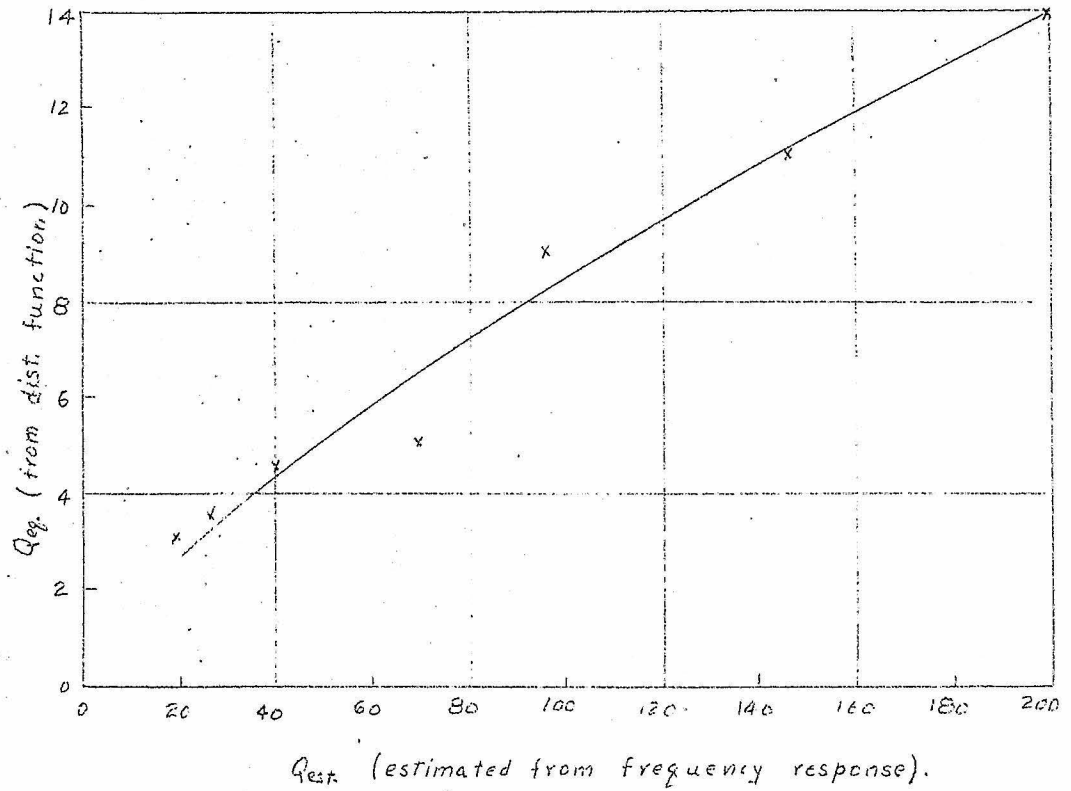


Fig. 36. The  $Q$  of the distribution function as a function of the  $Q$  estimated from the frequency response, bridged-T filters.

$$Q_1 = 100$$

$$Q_2 = 10$$

$$A_1' = 1$$

$$A_2' = .2$$

$$n = .708$$

$$Q_e = 17 .$$

This agrees fairly well with the value  $Q_e=14$  given by the distribution function.

To illustrate more clearly that broad spectra give broad frequency functions we can plot values of  $Q$  determined from the distribution functions against  $Q$ 's estimated from the filter characteristics. This is shown in Fig. 36 for the bridged-T sequence.

Conclusions. In retrospect it is easy to suggest improved means of procedure, particularly with regard to the equipment. Some of the components could be eliminated, and others improved. The use of blocking oscillators might combine several of the operations. The weakest parts of the system were the power supplies and the final clipping circuit. It remains to be seen whether the use of batteries for filament and plate in the early stages and noise source would remove some of the low frequency extraneous noise.

However the agreement between theory and experiment, in the regions where the theory was thought valid, was

satisfactory. The first term of the series for the frequency function, Eq. 2, appears to represent closely the frequency function, for narrow spectra.

Further research along these lines would include broad spectra, and perhaps evaluation of the second term of Eq. 2. The case of noise flat to a frequency  $f_0$  could be considered. Also there is the interesting problem of widely separated band-pass filters. Our results indicate that two closely spaced band-pass filters act as a single band-pass filter.

## REFERENCES:

1. Schottky, W., Ann. d. Physik (1918), v 57, p541.
2. Nyquist, H., Phys. Rev. (1928), v 32, p110.
3. Johnson, J. B., Phys. Rev. (1928), v 32, p97.
4. Landon, V. D., I.R.E. Proc. (1936), v 24, p1514.
5. Jansky, K. G., I.R.E. Proc. (1937), v 25, p1517.
6. North, D. O., RCA Review (1942), v 6, p332.
7. Landon, V. D., I.R.E. Proc. (1941), v 29, p50.
8. Rice, S. O., B.S.T.J. (1944), v 23, p97.
9. Middleton, D., J.A.P. (1946), v 17, p778.
10. Middleton, D., Q.A.M. (1948), v 5, p445.
11. Middleton, D., I.R.E. Proc. (1948), v 36, p1467.
12. Kac, M., and Siegert, A.J.F., J.A.P. (1947), v 18, p383.
13. Wiener, N., "Extrapolation, Interpolation, and Smoothing of Stationary Time Series", (1949), John Wiley and Sons.
14. Zadeh, L. A., and Ragazzini, J. R., J.A.P. (1950), v 21, p645.
15. Rice, S. O., B.S.T.J. (1944), v 23, p282.  
B.S.T.J. (1945), v 24, p46.
16. Franz, K., Elek. Nach. Tech. (1940), v 17, p215.
17. Wiener, N., Acta. Math. (1930), v 55, p117.
18. Ferrar, "Algebra", Oxford University Press.
19. Valley, G. E., and Wallman, H., "Vacuum Tube Amplifiers", (Radiation Laboratory Series, Vol. 18), McGraw-Hill Book Company, (1948).